AD-A112 300 NAVAL POSTGRADUATE SCHOOL MONTEREY CA F/G 20/3
ELECTRIC DISCHARGE FLOW INTERACTION IN PARALLEL AND CROSS-FLOW --ETC(U)
SEP 81 J W WAINIONPAA

UNCLASSIFIED NL

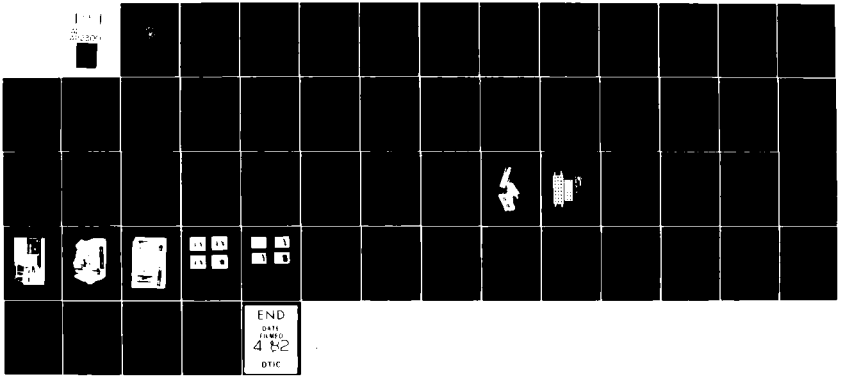

END
DATE FILMED
4 82
DTIC

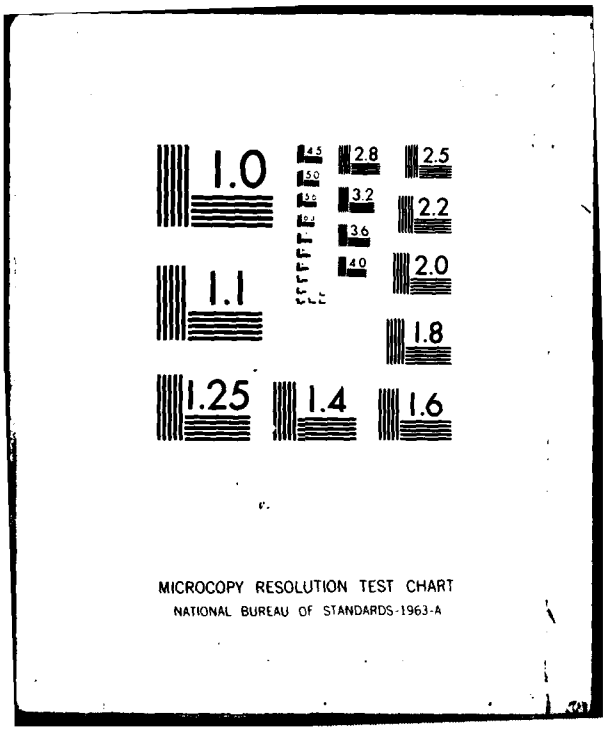
1.0
1.1
1.25
1.4
1.6
1.8
2.0
2.2
2.5
2.8
3.2
3.6
4.0
4.5
5.0
MICROCOPY RESOLUTION TEST CHART
NATIONAL BUREAU OF STANDARDS-1963-A

(2)

# NAVAL POSTGRADUATE SCHOOL
## Monterey, California

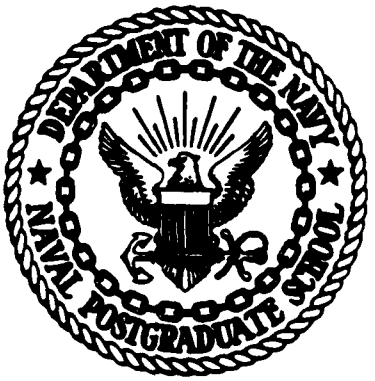


# THESIS

ELECTRIC DISCHARGE FLOW INTERACTION IN PARALLEL AND CROSS-FLOW ELECTRIC FIELDS

by

John William Wainionpaa

September 1981

Thesis Advisor: Oscar Biblarz



Approved for public release, distribution unlimited

SECURITY CLASSIFICATION OF THIS PAGE (When Data Entered)

| REPORT DOCUMENTATION PAGE | | READ INSTRUCTIONS BEFORE COMPLETING FORM |
|---|---|---|
| 1. REPORT NUMBER | 2. GOVT ACCESSION NO. AD-A112 340 | 3. RECIPIENT'S CATALOG NUMBER |
| 4. TITLE (and Subtitle) Electric Discharge Flow Interaction in Parallel and Cross-Flow Electric Fields | | 5. TYPE OF REPORT & PERIOD COVERED Master's Thesis; (September 1981) |
| | | 6. PERFORMING ORG. REPORT NUMBER |
| 7. AUTHOR(s) John William Wainionpaa | | 8. CONTRACT OR GRANT NUMBER(s) |
| 9. PERFORMING ORGANIZATION NAME AND ADDRESS Naval Postgraduate School Monterey, California 93940 | | 10. PROGRAM ELEMENT, PROJECT, TASK AREA & WORK UNIT NUMBERS |
| 11. CONTROLLING OFFICE NAME AND ADDRESS Naval Postgraduate School Monterey, California 93940 | | 12. REPORT DATE September 1981 |
| | | 13. NUMBER OF PAGES 57 |
| 14. MONITORING AGENCY NAME & ADDRESS(if different from Controlling Office) | | 15. SECURITY CLASS. (of this report) Unclassified |
| | | 15a. DECLASSIFICATION/DOWNGRADING SCHEDULE |

16. DISTRIBUTION STATEMENT (of this Report)

Approved for public release, distribution unlimited

17. DISTRIBUTION STATEMENT (of the abstract entered in Block 20, if different from Report)

18. SUPPLEMENTARY NOTES

19. KEY WORDS (Continue on reverse side if necessary and identify by block number)

discharge stabilization, parallel flow electric field, cross-flow electric field, turbulence, electrical lasers

20. ABSTRACT (Continue on reverse side if necessary and identify by block number)

This work deals with an evaluation of power capacity of two glow discharge orientations with respect to a flowing medium, namely, parallel and cross-flow. A test section was designed and fabricated to compare the effects of flow, turbulence generated by perforated plates, electrode spacing and electrode length on the cross-flow electric field to the performance of an existing parallel flow electrode set of the same type: positive pin-rack

DD FORM 1 JAN 73 1473 EDITION OF 1 NOV 65 IS OBSOLETE
S/N 0102-014-6601



SECURITY CLASSIFICATION OF THIS PAGE (When Data Entered)

(anode) and plane (cathode). Discharge data and photographs are presented.

Flow and turbulence are stabilizing. The parallel flow electric field discharge permits higher power than the cross-flow field. Increased cathode length in the streamwise direction produces a small detriment to discharge power.



A

Approved for public release, distribution unlimited

# Electric Discharge Flow Interaction in Parallel and Cross-Flow Electric Fields

by

John William Wainionpaa
Lieutenant Commander, United States Navy
B.S., University of New Mexico, 1972

Submitted in partial fulfillment of the requirements for the degree of

MASTER OF SCIENCE IN AERONAUTICAL ENGINEERING

from the

NAVAL POSTGRADUATE SCHOOL
September 1981

Author: John W. Wainionpaa

Approved by: Oscar Biblarz
Thesis Advisor

Chairman, Department of Aeronautics

William M. Tolles
Dean of Science and Engineering

## ABSTRACT

This work deals with an evaluation of power capacity of two glow discharge orientations with respect to a flowing medium, namely, parallel and cross-flow. A test section was designed and fabricated to compare the effects of flow, turbulence generated by perforated plates, electrode spacing and electrode length on the cross-flow electric field to the performance of an existing parallel flow electrode set of the same type: positive pin-rack (anode) and plane (cathode). Discharge data and photographs are presented.

Flow and turbulence are stabilizing. The parallel flow electric field discharge permits higher power than the cross-flow field. Increased cathode length in the streamwise direction produces a small detriment to discharge power.

TABLE OF CONTENTS

I. INTRODUCTION ---------- 8

II. EXPERIMENTAL APPARATUS ---------- 12

A. FLOW EQUIPMENT ---------- 12

B. DISCHARGE CIRCUIT ---------- 14

III. RESULTS ---------- 18

A. GENERAL ---------- 18

B. PARALLEL FLOW ---------- 21

C. CROSS-FLOW ---------- 23

IV. CONCLUSIONS ---------- 27

V. RECOMMENDATIONS ---------- 29

LIST OF REFERENCES ---------- 54

INITIAL DISTRIBUTION LIST ---------- 56

LIST OF FIGURES


| Figure | | Page |
|---|---|---|
| 1. | Air flow system schematic | 33 |
| 2. | Discharge electrodes, parallel flow | 34 |
| 3. | Turbulence generating screens | 35 |
| 4. | Breakdown voltage as a function of electrode geometry | 36 |
| 5. | Pin anode, parallel flow | 37 |
| 6. | Pin anode, cross-flow | 38 |
| 7. | Cathodes, cross-flow | 39 |
| 8. | Laboratory setup | 40 |
| 9. | Parallel flow test section | 41 |
| 10. | Cross-flow test section | 42 |
| 11. | Cross-flow glow discharge, 2.9 cm spacing | 43 |
| 12. | Cross-flow glow discharge, 4.1 cm spacing | 44 |
| 13. | No-flow breakdown voltage versus spacing | 45 |
| 14. | Parallel flow discharge power versus velocity, with turbulence | 46 |
| 15. | Parallel flow discharge power versus velocity, no turbulence | 47 |
| 16. | Cross-flow discharge power versus velocity, no turbulence | 48 |
| 17. | Cross-flow discharge power versus velocity, with turbulence | 49 |
| 18. | Breakdown current versus flow velocity | 50 |
| 19. | Glow discharge variation with voltage | 51 |
| 20. | Glow discharge sketch | 52 |
| 21. | Power versus spacing, no flow | 53 |

ACKNOWLEDGMENT

The author gratefully wishes to thank the many people concerned with the successful completion of this work, in particular: Associate Professor Oscar Biblarz for his guidance, support and the original inspiration of the study; the technical staff of the Department of Aeronautics under Bob Besel and Ted Dunton, especially Glen Middleton and Ron Ramaker for their expertise in the fabrication and modification of the experimental apparatus; Heidi, Erik and Sinikka Wainionpaa for their unwavering faith; and most importantly my wife Linda for her steadfast love and constant encouragement.

# I. INTRODUCTION

Many applications exist where maximum diffuse power is desired between electrodes immersed in, or separated by, a gaseous medium; for example, magnetohydrodynamic power generation, plasma chemistry devices, and electrically pumped lasers. Increases in power are desired over currently obtainable values. However, the power may not be increased without bound merely by increasing the applied electric field, nor by changing spacing or electrode sizes. The limiting factor to maximum obtainable power is the arc discharge through the medium, wherein the resistance and dielectric strength diminish precipitously, high current flows (generally very localized), the electric field collapses, and damage to electrode surfaces can occur. The gaseous medium itself, the material and geometry of the electrodes, and the conditions of flow all markedly influence the onset of arcing.

Several different electrode configurations are reported in the open literature, which include parallel (axial) and cross-flow electric field configurations. Since much cooling can be achieved by the parallel flow configuration, with almost the entirety of the electrodes immersed in the flow, it is desirable to know the power advantages of this over the cross-flow configuration where the electrodes form part of the walls. Clearly, with the electrodes across the flow,

less blockage due to the electrodes is encountered. Also, the extent of the electric field in the streamwise direction and length of the electrodes is limited by the length of the reacting chamber, whereas the height or width of the cross-section limits the maximum dimension of the parallel flow electrodes. An attempt is made here to weigh the relative merits of these two flow configurations with common positive pin-rack electrode and flat plane cathode designs.

Optimum power for given spacings has been determined elsewhere as a function of pressure, but the reported pressures are extremely sub-ambient and the larger the gap, the lower the pressure required [Ref. 1]. The experiments conducted for this work are at atmospheric pressure.

Though the examples of magnetohydrodynamics and plasma chemistry have been cited, this work is part of a continuing investigation at the Naval Postgraduate School into phenomena affecting optimization of the Electric Discharge Convection Laser (EDCL) power-handling characteristics.

It has been learned that the EDCL is capable of high power output, though it is limited by the amount of electrical power coupled into the laser cavity [Ref. 2]. Laser gain is proportional to the population inversion, which in the EDCL is created by the pumping due to the applied electric power flowing in the cavity. Hence, the greater the power capable of being coupled into the laser cavity, the greater the possible output. The limiting factor is the electrical

constriction of the gaseous discharge or arcing, the resulting low-resistance path for current, and the ensuing collapse of the applied electric field which can then no longer pump the laser.

Numerous studies have proven the positive effects on stabilizing the electrical discharge by convection and turbulence, both of which significantly raise the power-handling capacity of the laser medium by delaying the arc-breakdown. Discharge power in excess of two hundred times that for a static medium has been shown possible by the convection of a flowing medium [Refs. 3 and 4]. Further enhancement of the power capacity has been demonstrated by conditioning the flow with turbulence-generating screens [Refs. 4 and 5].

A mathematical model accounting for the effects of both convection and turbulence independent of one another has been proposed by Barto in Reference 5. The present work is an attempt to provide experimental data in support of that model and to investigate phenomena such as coloration of the discharge, sparking but not breakdown in the discharge, downstream effects of an additional cathode, cross-flow and parallel-flow power capabilities, and pin discharge characteristics with increasing flow.

The experiments are conducted using flow in a non-recoverable system. Since the flowing medium is discharged and lost to the atmosphere; since the length of time required

to gather breakdown data is considerable (in part attributable to the effects of the time rate of change of applied field voltage on arc breakdown [Ref. 5]); and since the cost of unrecovered flow of large quantities of laser mixtures is prohibitive, the medium used is air from an existing flow system, discussed in the next section. Moreover, discharges in air are sufficiently challenging because of the complex chemical activity of the medium. No attempt is made to lase the medium in this work.

## II. EXPERIMENTAL APPARATUS

The experimental apparatus consists of two main systems: the flow equipment to develop and condition the flow of air through the discharge gap; and the high-voltage discharge circuit to develop the electric field between the discharge electrodes. The discharge circuit also provides for the measurement of the voltage across and the current through the discharge.

### A. FLOW EQUIPMENT

Flow is provided through the system originally designed for the research of Reference 4 and subsequently used in the work of References 3, 5 and 6. Modification for research in this work included fabrication of a new test section, electrodes and a turbulence generating screen compatible with the existing converging nozzle and the new test section.

The flow system consists of an air compressor, water-cooled heat exchanger, flow rate control valves, a plenum chamber, a converging nozzle to the test section, and turbulence generating plates. Air is exhausted directly to the atmosphere from the constant-area test section. Figure 1 shows the flow system schematically [from Ref. 3, modified].

Air is provided by a three-stage Carrier centrifugal compressor with a 4000 cubic feet per minute capability at

two atmospheres maximum pressure, through a water-cooled heat exchanger which maintains flow temperature at approximately 90°F, through an impact-type water and particle separator. Flow can be regulated by three gate valves (5, 6 and 7 in Figure 1). Only valves 6 and 7 were used in the experiments described herein, so that the full effect of the impact separator would be utilized. Flow velocities to 100 meters per second are obtainable by using just these two valves.

Air flow was measured by a pitot-static probe (connected to a mercury manometer) inserted in the exhaust opening of the test section. The probe was removed prior to applying power for discharge measurements.

From the results shown in Reference 6 and other recent works it is known that the aerodynamic source of turbulence should be placed as near as possible to the discharge region so as to optimize turbulence stabilization of the discharge. Therefore for the parallel flow case the turbulence generating plate (or "screen") of Reference 3 is used, since the plate is mounted directly on the anode support and separated from the discharge region by only the length of the anode pins (Figure 2).

For the cross-flow case a conflict arises. The most effective compromise between the desire to place the turbulence plate as close as possible to the anode and the need to keep from introducing either an insulator or a

conductor into the discharge gap itself was to mount the turbulence plate to the face of the test section. The cross-flow turbulence plate (Figure 3) has the same blockage (50%) and hole configuration as that of the parallel-flow plate, but in order to be supported it must span the width of the entry to the test section. Since this plate does not span the height of the opening, high-speed boundary-layer slots similar to those provided by the smaller parallel-flow plate exist. This, too, is desirable to keep conditions equivalent to previous work.

The cross-flow (new) test section differs from the parallel-flow (old) test section in two ways: in the orientation of the electrodes with respect to the flow, and in the length. The cross-sectional areas are identical (2.22 x 4.44 inches) and constant. The cross-flow test section is longer than the parallel-flow section so as to accommodate the downstream cathode.

## B. DISCHARGE CIRCUIT

The discharge circuit consists of a high voltage power supply, high voltage leads, current and voltage instrumentation, the pin-rack anodes and the "plane" cathodes.

The power supply is a Universal Voltronics Labtrol Model BA 50-70 which provides up to 50 kilovolts and 70 milliamperes direct current, a significant increase over capabilities available to previous researchers utilizing

this flow system. The power supply consists of a control unit and a high-voltage output cannister. The control unit houses a voltmeter and an ammeter and is internally regulated and limited to break the circuit when either the output voltage exceeds 50 kilovolts or the current supplied exceeds 70 milliamperes. Provision for lowering the trip voltage or current is available. In addition to the sight and sound of arcing across the electrodes, the current-limiting feature serves as confirmation of the electric discharge breakdown, i.e., when the trip current is exceeded the power supply shuts off and the panel lights indicate an overload. This feature proves to be a definite factor in protecting backup current meters in the circuit. The two components of the power supply are connected by manufacturer-supplied cables. The output of the high-voltage cannister is connected to a polished, high-voltage sphere by a factory-supplied high-voltage cable.

Locally-prepared high-voltage leads to the laboratory voltmeter and anode are then connected to the high-voltage sphere which is immersed in a high-dielectric oil bath to prevent arcing. Cathode-to-ground connections are also locally-prepared high-voltage leads. For safety, all equipment is well-grounded through a common laboratory ground.

Anode design is three rows of thirteen stainless steel pins, unballasted, and connected in common. As is apparent

from Figure 4, the positive-pin-to-negative-plane configuration provides the lowest breakdown voltage for a given spacing in air. This is desirable so as to induce breakdown within the limitations of the available power supply. The power-handling capacity of the various electrode shapes can then be compared once the breakdown mechanism is understood. Figures 5 and 6 show the two types of pin mounts used in this work.

In both parallel and cross-flow experiments the anode is fixed and spacing is varied by moving the cathode(s). The length of the cross-flow pins is such that they protrude into the flow far enough (0.25 inch) for the pointed tips to be out of test-section wall boundary layers at flows as low as 0.1 meters per second.

The dimensions of the cathodes are 2.22 x 4.44 inches. Thus the parallel-flow, brass grid of airfoils (shown in Figure 2) fills the entire cross-section of the test section, effectively presenting a plane of ground potential to the anode, yet allowing minimum blockage of flow. This is a common electrode configuration in parallel-flow systems.

The cathodes of the cross-flow experiments are shown in Figure 7. Both are constructed of stainless steel. The upstream cathode is centered below the anode to given an electric field and corona discharge pattern equivalent to that of the parallel-flow setup under no-flow conditions.

The downstream cathode is supported by strips of fiberglass-reinforced phenolic and epoxy bonded to the upstream electrode. These strips also serve to electrically insulate the two electrodes, while providing parallel motion during electrode spacing adjustment.

Stainless steel was chosen because it is locally obtainable, relatively easily machined, and yet exhibits a high resistance to erosion from electrical currents.

Voltage applied is measured by a Sensitive Research 0-40 kilovolt meter with an input impedance of $5 \times 10^{15}$ ohms, and cross-checked with the voltmeter on the power supply. Total current through the discharge is measured by the power supply milliammeter, and the downstream current is measured with a Hewlett-Packard 3469B calibrated digital multimeter.

Figure 8 is a photograph of the laboratory setup. The cross-flow test section is visible behind and between the power supply control panel (right) and the multimeter (center).

Figures 9 and 10 allow comparison of the test sections, and illustrate the placement of the electrodes. Flow is from left to right in both photographs.

# III. RESULTS

## A. GENERAL

The fabrication of the new electrodes and test section and the introduction of the new power supply into the existing system necessitated a validation of system performance by comparison of present results to those obtained by previous researchers who used the same flow system and combinations of the same parallel flow electrodes.

Electrode surfaces were cleaned by sandblasting and wiping with evaporative solvents (denatured alcohol and carbon tetrachloride). The desired test section was connected to the flow system with or without turbulence generating plates. Then applied field voltage and current data up to and including breakdown were taken, at different air flow rates and various interelectrode spacings.

Late in the experimental effort, photographs of the discharges were taken.

Overall performance of both sets of electrodes, parallel and cross-flow pin-rack anodes and plane grid or plane cathodes, was judged to be excellent, based on the following. Figures 11 and 12 together with 35-millimeter slides were taken of the glow discharges with the laboratory darkened. An even, round, pinkish-orange glow was evident at the tipmost third of the conical end of each pin of both anodes, in both flow and

no-flow conditions. The glow discharges visible in both parallel flow and cross-flow configurations' no-flow conditions (as in Figure 12a) were symmetric about the center row of pins, and identical in appearance with regard to the intensity, color, width, diffuseness and shape of the glows for the same interelectrode gap dimension. This similarity of glow discharges was especially heartening confirmation of the assumption that the grid cathode of the parallel flow equipment functions as if it were an entire plane of ground potential (where the cross-flow cathode is in fact a plane surface) and also proof of the equivalency of the two anodes' performance.

Before beginning the experiments of this work, it was felt that a single arc would be the most likely mechanism of arc breakdown. The 35-millimeter slides (which were taken for a separate study) showed, however, from six to nine arcs, which spanned the interelectrode gap, to be active at breakdown. These breakdown arcs appeared to originate randomly from different pins in the pin-rack anodes in both flow and non-flow conditions, and in both parallel and cross-flow configurations. This randomness is further confirmation that the breakdown is electrical in nature, and not a function of effects dominated by a single misaligned pin or group of pins.

The cathode performance of the parallel flow test section had been ascertained by the research of Davis in Reference 6,

but the cross-flow cathodes' performance was subject to verification. At first, the two cross-flow cathodes appeared to function independently at all power levels. However, the darkened laboratory experiments and Figures 11 and 12 show discharges in the lower left corner of the photographs between the primary and the downstream cathode at higher power levels. Thresholds of this effect were not determined for this work. The inter-cathode discharging is not limited to one place on the adjacent cathode plates, but rather several arcs occurred at random positions across the width of the test section, that is in the direction perpendicular to the plane of the photograph. The arcs were evident whether or not the downstream cathode was connected to laboratory ground. A possible explanation of this phenomenon follows.

The current in this diffusion-dominated discharge is mainly due to electron flow from the cathode across the interelectrode gap to the anode. When the downstream cathode reaches a potential such that the dielectric strength of the air and epoxy insulation between cathodes is exceeded, arcing from the downstream to the upstream cathode becomes visible. The recombination region above the downstream cathode causes its potential rise, because there measurable electron-ion pairs are neutralized, [Ref. 5] some of the electrons having been drawn from the downstream cathode. (The subject of these arcs will be readdressed in the Recommendations Section of this thesis.)

The parallel flow observations will be discussed next and correlated with earlier work to verify performance, reliability, and usefulness of data. A discussion of the results obtained using the new cross-flow test section follows.

B. PARALLEL FLOW

From Figure 4 (von Engel), the no-flow arc breakdown voltage for a spacing of 2.9 centimeters is approximately 27 kilovolts in the positive-pin-to-negative-plane electrode configuration. This is consistent with the results reported by Post and Barto who used aluminum honeycomb as the negative plane [Refs. 3 and 5]. However, results of this present study which used the multiple-pin anode of Post and Barto and the cathode of Reference 6, were significantly lower: 21.5 to 23 kilovolts.

In light of the marked difference, the first concern was to verify the voltmeters' calibrations. Such a large discrepancy could not have arisen from the $\pm$0.1 kilovolt gauge reading error. The power supply voltmeter was a maximum of 0.4 kilovolts lower than the Sensitive Research kilovoltmeter while being calibrated on the same scales. The voltmeters were judged to be not the source of the difficulty.

The next question relates to effects of the change in electrode material on the breakdown voltage: Is the aluminum cathode of Post and Barto so significantly different from the

present brass cathode? Reference 8 flatly states, "At atmospheric pressure the sparking potential has been found to be largely if not entirely independent of cathode material." Nonetheless, the open literature has a wide disparity in accepted no-flow breakdown voltages for the positive-pin-to-plane in air at standard temperature and pressure (STP), as shown in Figure 13. A correlation between the present experimental results and the results of Reference 6, both of which utilized the same brass cathode, was unobtainable due to the paucity of documentation of interelectrode gap dimensions. As a result, no conclusive explanation is available for the lower breakdown voltage.

This present study is concerned with comparison and enhancement of the available system, and much of the analysis was non-dimensionalized or used only on a relative basis, so it was assumed that the present results are correct for this configuration and equipment. The values thus obtained were applied to the non-dimensional theory of Reference 5. (Another disparate result in the form of a still lower no-flow breakdown voltage for the same gap in the cross-flow configuration (19-19.5 kilovolts) will be addressed in the next section).

Figures 14 and 15 are plots of the parallel flow maximum power input (i.e., just prior to arc breakdown) as a function of flow velocity, with and without turbulence. As anticipated, power increases as the air flow increases, and

additional power capacity is obtained with the introduction of the turbulence generating plate.

The results obtained in the parallel flow configuration thus bear out previous findings regarding at least the trends of performance enhancement by flow conditioning, if not the numerical results.

## C. CROSS-FLOW

The first result of the cross-flow experiments, as noted above, was the lower no-flow breakdown voltage. In view of the sparking observed between the cathodes, it would be well to investigate the effects of a single 2.22 x 4.44 inch cathode, to more closely simulate the parallel flow electric field geometry. (Further research into cathode geometry is suggested in the Recommendations section.) The lower breakdown voltage is somewhat of a puzzle since when the downstream cathode is active in the discharge, the electric field across the gap is distributed over a larger area, and hence less concentrated at the pins. It would appear, therefore, that the breakdown voltage should be higher, not lower.

Figures 16 and 17 are plots of the maximum power as a function of flow velocity for the four spacings 2.5, 2.9, 3.5 and 4.1 centimeters, without turbulence in the flow (Fig. 16) and with the turbulence plate installed (Fig. 17). Since the primary goal is the optimization of discharge

power, only the results of the single, primary cathode experiments are shown here; for all spacings and conditions of flow, the power available into the discharge was greater when the downstream electrode was not grounded. The field breakdown voltages were not significantly changed by the grounding of the downstream cathode, however, the current supplied to the discharge was somewhat lower, hence the power decrease. Contrary to expectations, the increase in surface area by addition of another cathode actually decreases the power in the discharge.

The predicted result of increased stabilization of the discharge by flow of the medium is observed in all cases. In general, the faster the flow, the greater the power into the discharge. A nearly linear increase in power with flow velocity is observed in the case of the 2.9 centimeter gap, single cathode, no turbulence plate; other increases occur at a rate generally greater than linear.

Turbulence further stabilizes the discharge for the spacings 2.5, 2.9, and 3.5 centimeters, but the discharge power with turbulence for 4.1 centimeters is less than that for without turbulence. A study of the velocity profiles might reveal some pertinent information.

Comparing Figures 16 and 17 to 14 and 15 it is readily apparent that the parallel flow configuration has the higher power capacity than the cross-flow, with the notable exception of the 4.1 centimeter gap at 55 meters per second

with no turbulence plate. The downstream cathode current increases at a slower rate than the total discharge current with increasing flow, as is evidenced by Figure 18. The surface (boundary layer, secondary emission, and thermionic emission) effects most probably dominate here so that convection turns out to have a less pronounced effect.

Part of the difficulty in attaining greater power capacity with the cross-flow configuration arises from the position of the turbulence plate. Different turbulent intensity is present over each row of anode pins. The row of pins farthest upstream has the greatest turbulence acting upon it, with the downstream rows having progressively less. This explains the marked growth of the upstream row's glow compared to that of the downstream rows.

The characteristic behavior in the glow discharge in a flow with increasing applied voltage can be described by reference to Figure 19. Consider the pin rows numbered from 1 to 3, 1 being the upstream row. When the corona first becomes visible, the glow extends from row 1 almost antiparallel to the flow, tilted slightly toward the cathode. As voltage increases, the glow from row 1 bends downward and a glow begins at row 3. Further voltage increases cause the glow from row 3 to become nearly as bright as that from row 1, and the side view of the discharge is symmetric with respect to row 2, and with only a faint glow from the center row. All the pin tips have the round pinkish-orange glow at this

point. Higher voltage causes the row 1 glow to become more dominant; the glow of row 2 increases in width and brightness; and row 3 diminishes in intensity. Just prior to arc breakdown, almost no glow is visible from row 3 except that at the very tips of the pins. At this point, streamers or sparks become visible in the row 1 glow, but they are not strong enough to cause the arc breakdown [Ref. 5]. (These breakdown streamers have been observed elsewhere [Ref. 12].) Increasing the voltage more, breakdown occurs.

Figure 20 depicts the impending breakdown cross-flow glow discharge. The colors reported in Reference 5 were again noted in this work and may be correlated to the characteristic colors of the constituents of the flowing air as described in Reference 13, and tabulated on the figure.

To delay the arc breakdown by eliminating some of the ionization products in the electrode gap, a small muffin fan was employed, blowing in the reverse direction from the normal flow, at an air flow speed too small to be measured by the pitot tube and mercury manometer. Results summarized on Figure 21 indicate an increase in power with increased electrode spacing. This is a fundamental improvement over the decreasing behavior of the parallel flow power or the widely fluctuating cross-flow performance.

## IV. CONCLUSIONS

Ultimately, as was stated in the introduction, the desired result is to increase the power input to the discharge. Given the present equipment, the maximum power available is for the parallel flow configuration, maximum interelectrode gap of 4.8 centimeters at a turbulent flow of approximately 60 meters per second. This is approximately 50% greater than any nearest competitor.

In all experiments, flow enhanced discharge stabilization, as did the introduction of turbulence, and the upper limit on parallel flow power capacity was due to the inability to increase gap length.

The appearance of cross-flow discharges reported in Reference 5 was confirmed in this work with the additional analysis of the observed colors as delineated on Figure 20.

The no-flow discharge power plotted as a function of electrode spacing in Figure 21 appears to show no correlation to the maximum power attained by flow conditioning, save that the configuration which yields the maximum power (parallel flow) is the same.

The addition of the downstream cathode into the system proved to be a detriment to cross-flow power capacity. Not only was the system with two cathodes connected unable to maintain the same power levels as the parallel flow arrangement,

but it was also less efficient than with just the one cathode. The increase of downstream current occurs at a slower rate than the total current increases with flow velocity, causing the deterioration in performance.

## V. RECOMMENDATIONS

The results of the efforts described in this work are one step in a growing body of knowledge of the equipment, phenomena, and procedures requisite for meaningful improvement in EDCL performance. To further the goal, the following modifications and considerations are offered as suggestions.

The darkened laboratory utilized in later stages of this work provided the opportunity to observe and photograph arcing between the upstream and downstream cathodes even when the downstream cathode was not connected by cable to ground. It is hypothesized that the recombination region of Figure 20 downstream of the anode provides the return current path. Two possibilities for investigation are suggested by the above: improve the insulation between the upstream and downstream cathodes by use of a different dielectric bonding agent between them and/or increasing the spacing greater than the present 0.1 inch; make current measurements connecting only the downstream cathode to ground.

Additional photographic analysis of the discharge in the darkened laboratory could document the perceived randomness of anode pin breakdown activity.

The increase of downstream current with increasing voltage is not surprising, however it is felt that time

studies of the downstream current using an oscilloscope could yield deeper insight into the onset of breakdown due to streamer instability production. Also any increase in streamer activity with time would be graphically shown on the oscilloscope screen, as the applied voltage approached breakdown voltage, enhancing the ability to pinpoint impending breakdown.

In the cross-flow configuration, the greater power load borne by the upstream row of anode pins with increasing flow and voltage applied evidenced by the glow photographs of Figures 11 and 12 suggests that though individually ballasted pins might be inappropriate due to their unwieldiness, lack of calibration, and expense, it might be advantageous to ballast each row of pins, with the upstream row assigned the highest resistance (the NASA High-Power Carbon Dioxide Laser utilizes both pin and row ballasts [Ref. 14]). Additional measurement techniques would then be required to determine the power developed in the discharge gap. The electrical efficiency of the discharge might decrease due to the power consumed in the ballast resistances, but the electric field and/or the discharge could be more uniform in the cross-flow gap.

In the area of turbulence generation, a more efficient means of creating turbulent and/or vortex stabilizing flow in the electrode gap must be found. In the cross-flow configuration, the distance between the turbulence screen

and the active electrodes is on the order of two inches. The best results for screen-generated turbulence were found in Reference 6 to be on the order of one-eighth inch, and scaled with velocity of flow, according to Reference 9.

Humidity is a significant factor in breakdown-causing instabilities [Ref. 15]. A standard of humidity compensation should be devised for this equipment. The no-flow discharge data are taken at ambient temperature, pressure, and humidity. The air in the discharge under flow conditions is compressed, cooled, dehumidified and scrubbed by the impact separator before acceleration through the converging nozzle to the test section. Non-dimensionalization of discharge parameters is accomplished by dividing the flow breakdown data by the no-flow values. It was originally thought that the humidity correction [Ref. 15] was equally applied to both numerator and denominator, but upon reconsideration, there were no diagnostics of the humidity or temperature (nominally 90°F through the effects of the heat exchanger) of the flowing air, while the ambient humidity and temperature of the laboratory still air varied significantly during the experiments (32 to 60 percent relative humidity and 62° to 76°F).

At the disassembly of the test equipment for photography, a layer of dustlike particles was observed on the turbulence screens and electrodes. It would be advantageous to analyze

the particles to determine their composition. Then, spectrophotographic analysis of the discharge, particularly at breakdown, would be a relatively simple method to determine whether the observed particles were reacting in the breakdown. This is less desirable than eliminating the airborne particulates totally, however the sheer logistics of clearing the flow system, while still remaining accessible to other users of the compressed air, are difficult. Installation of a more efficient separator may be required, or a filter installation between the existing impact separator and the plenum chamber of Figure 1.

Finally, to address the problem of cathode similarity, it might be advantageous to compare the breakdown characteristics of a grid, identical to the parallel flow cathode, but embedded in a smooth surface, as the cross-flow cathode. This would eliminate doubt as to the validity of direct comparison of parallel and cross-flow results, especially in view of the deleterious effects of the added surface area of the downstream cathode.

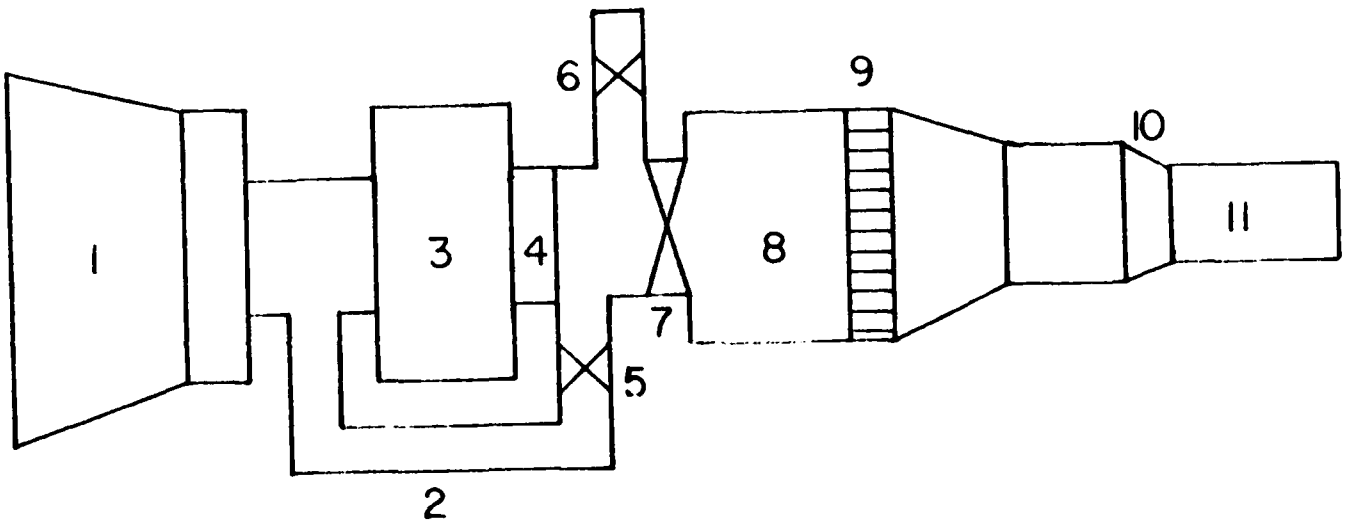


1. Compressor
2. Heat Exchanger Bypass
3. Heat Exchanger
4. Water Separator
5. Gate Valve
6. Gate Valve
7. Gate Valve
8. Plenum
9. Honeycomb
10. Converging Nozzle
11. Test Section

Figure 1. Air flow system schematic

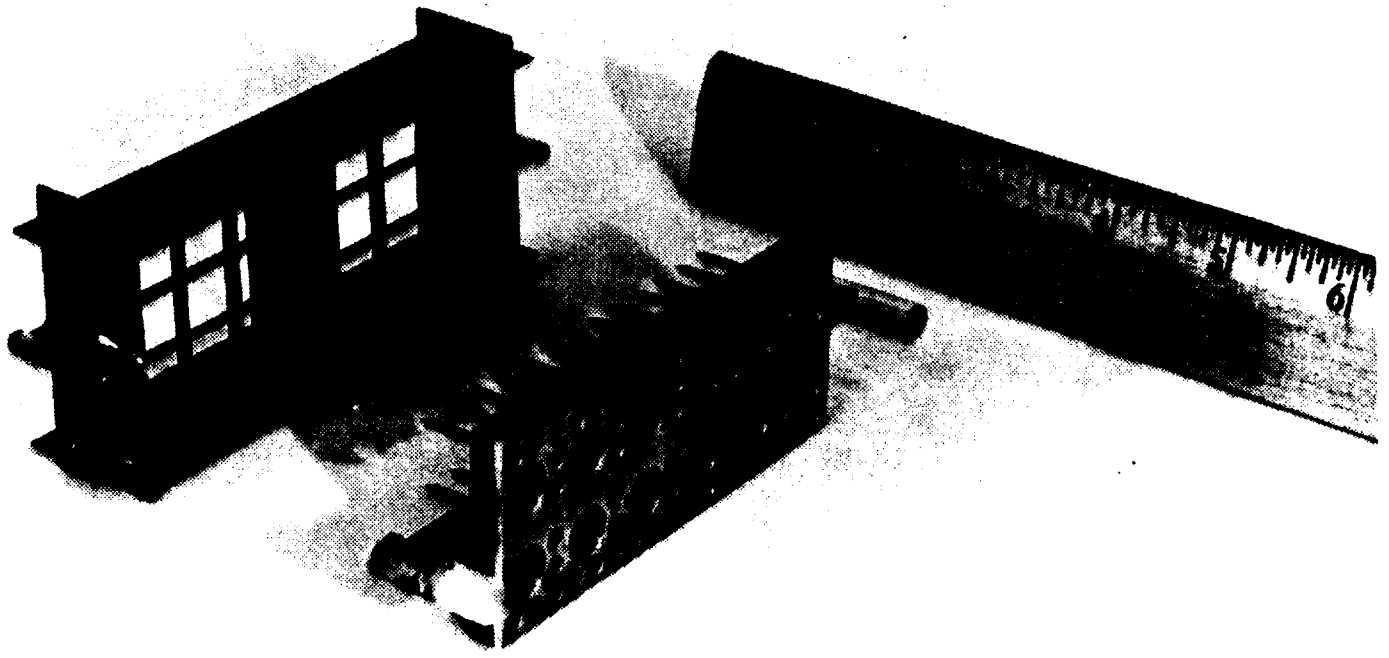

Figure 2. Discharge electrodes, parallel flow

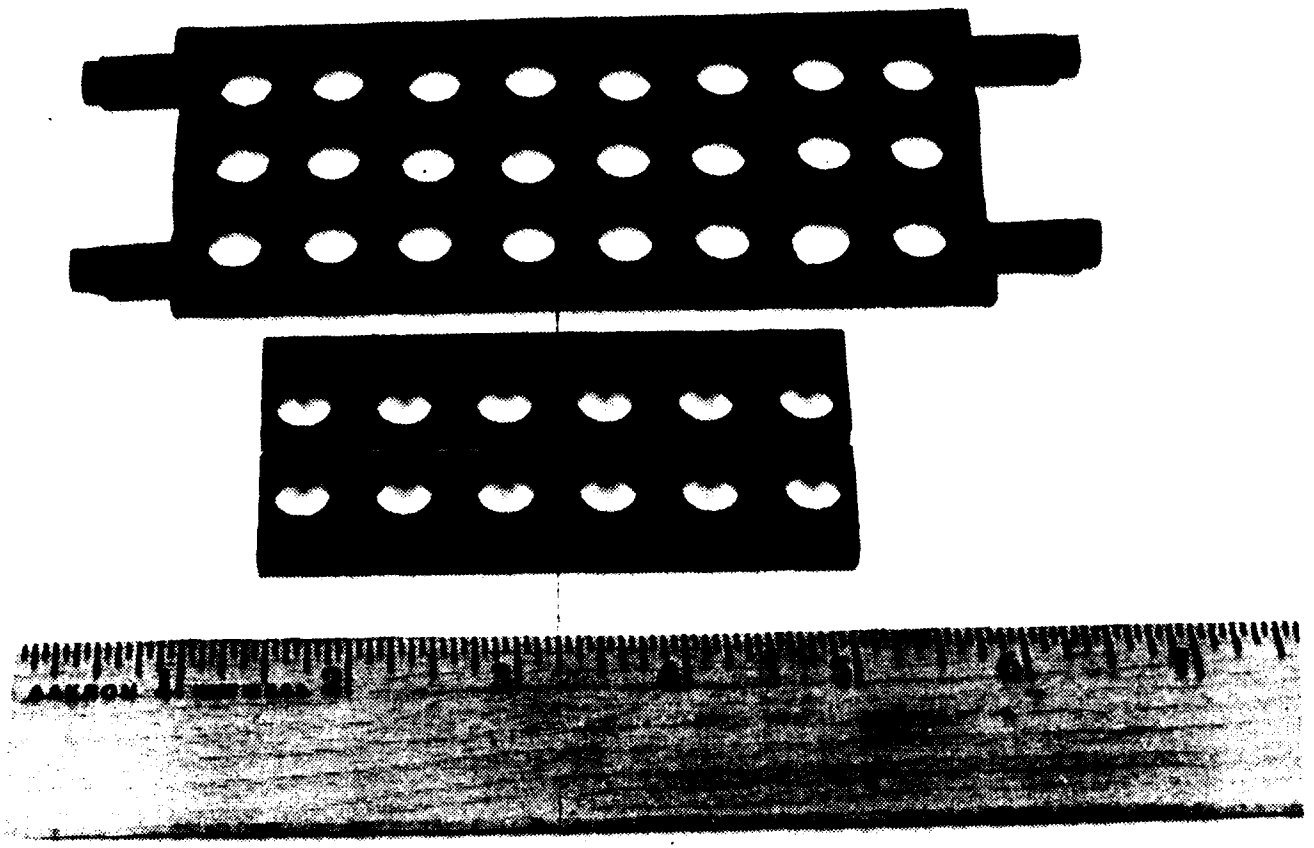

Figure 3. Turbulence generating screens: cross-flow (top) and parallel flow (bottom)

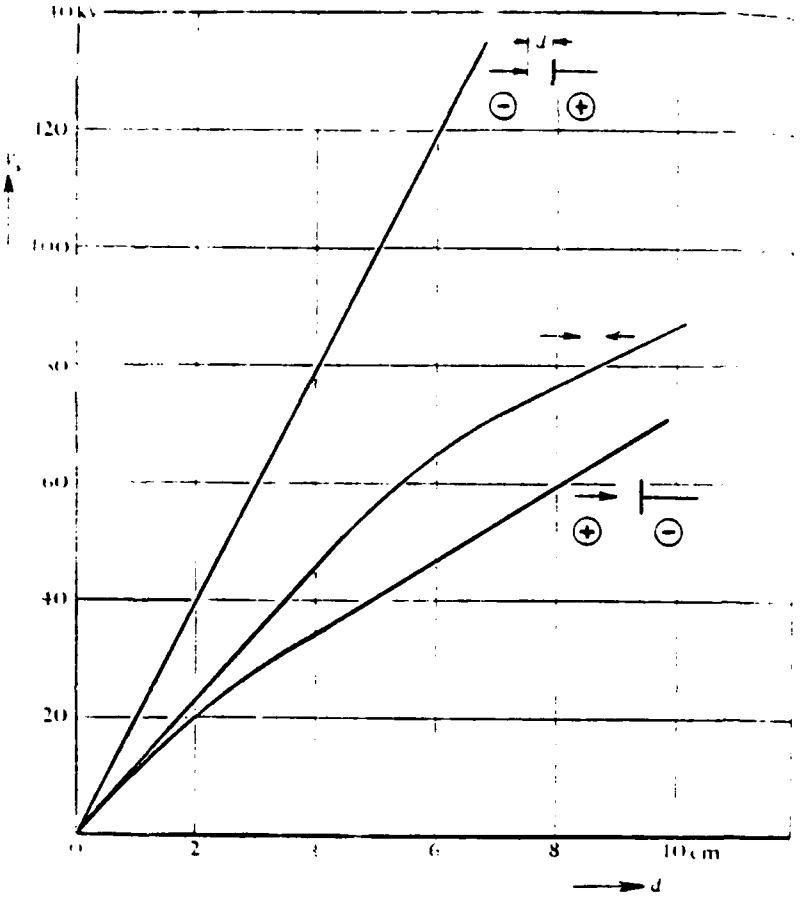


Figure 4. Breakdown voltage as a function of electrode geometry (in air at s.t.p., 30 percent humidity [Ref. 7]).

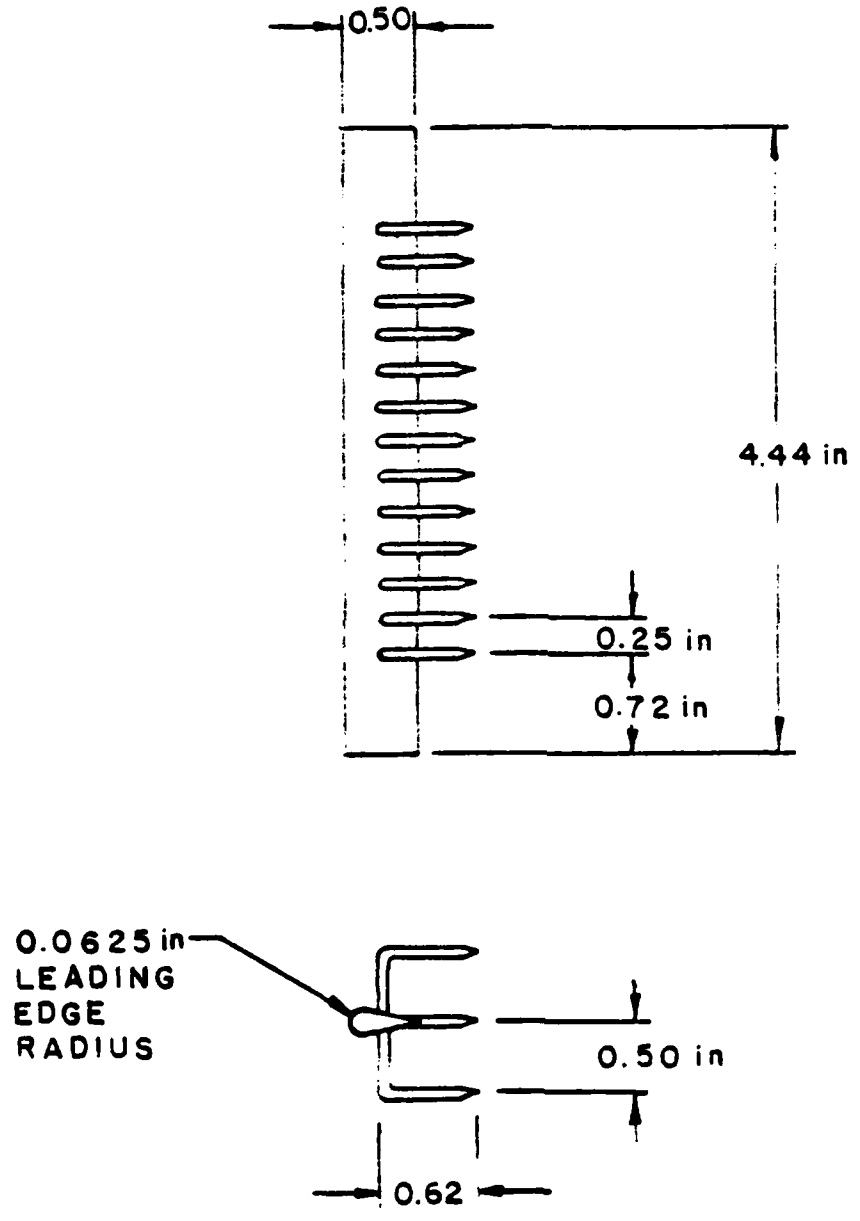


Figure 5. Pin anode, parallel flow

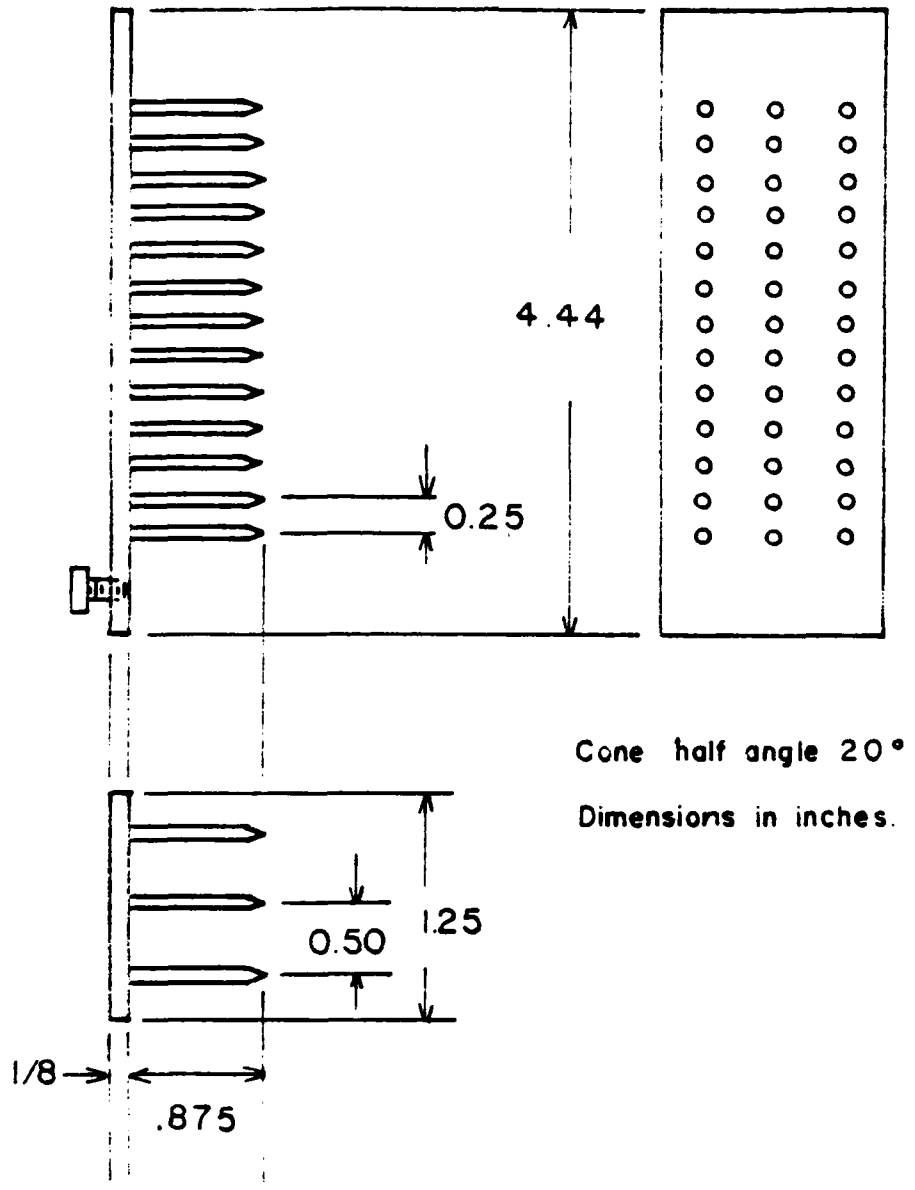


Figure 6. Pin anode, cross-flow

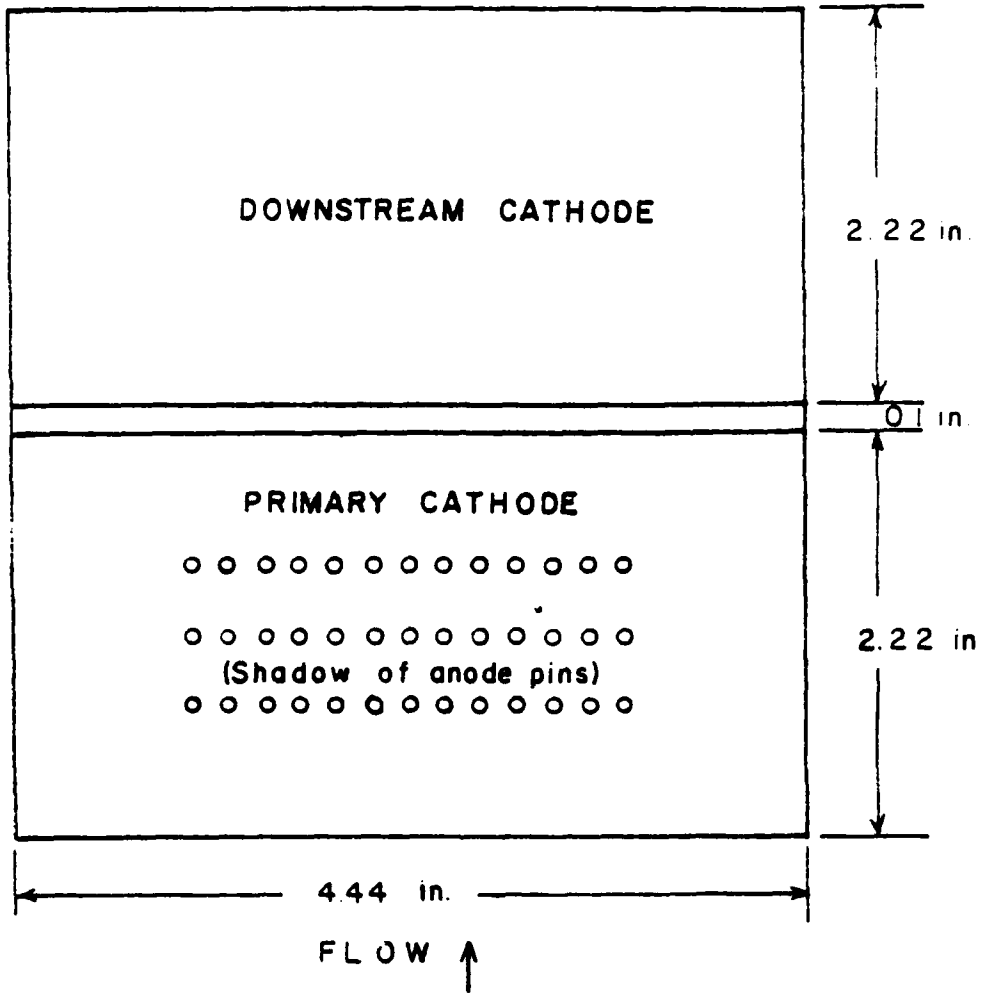


1/16 in. Stainless steel

Anode pins shown viewed from top.

0.1 inch insulator of phenolic

Figure 7. Cathodes, cross-flow

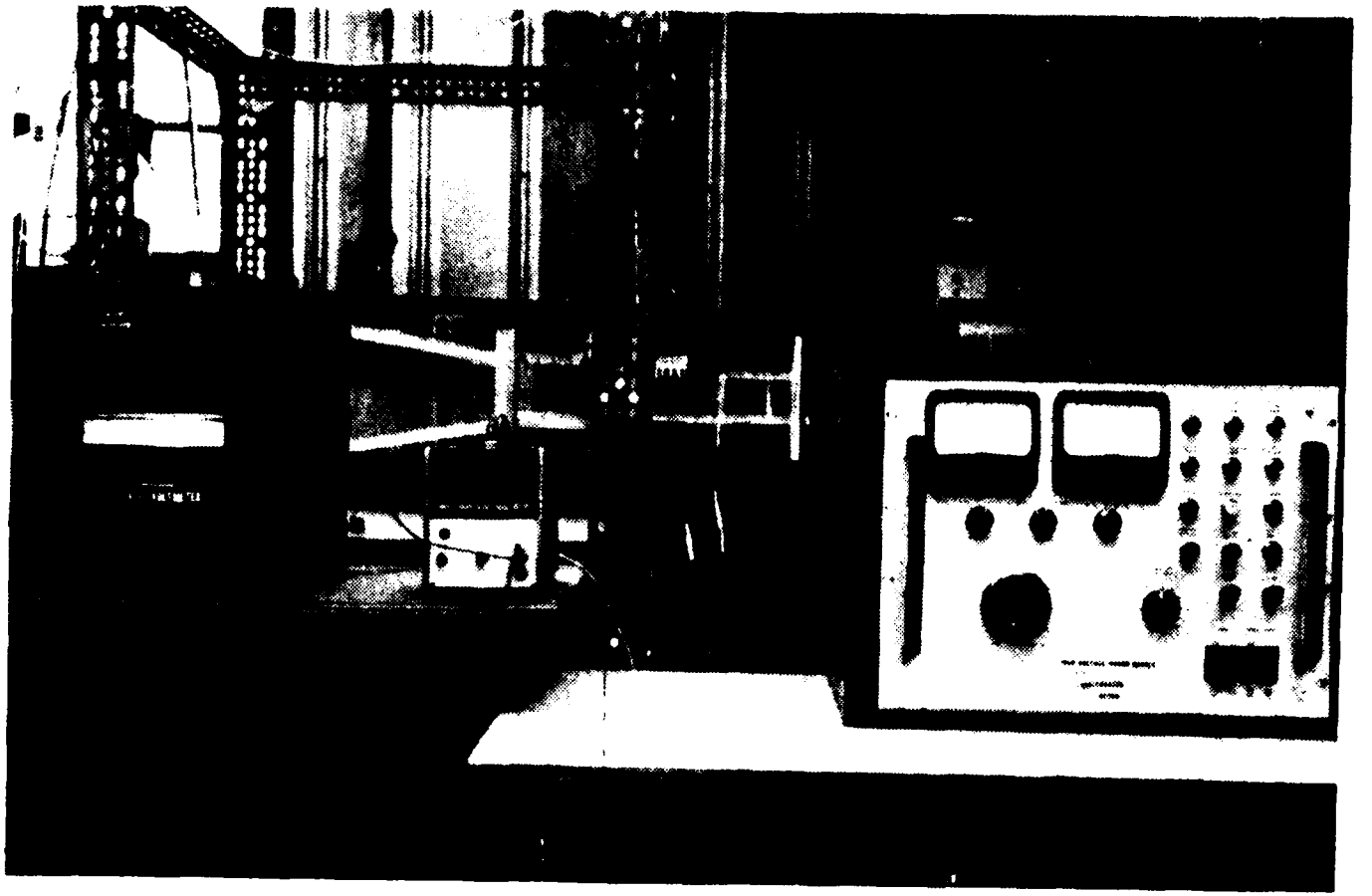

Figure 8. Laboratory setup, cross-flow test section installed

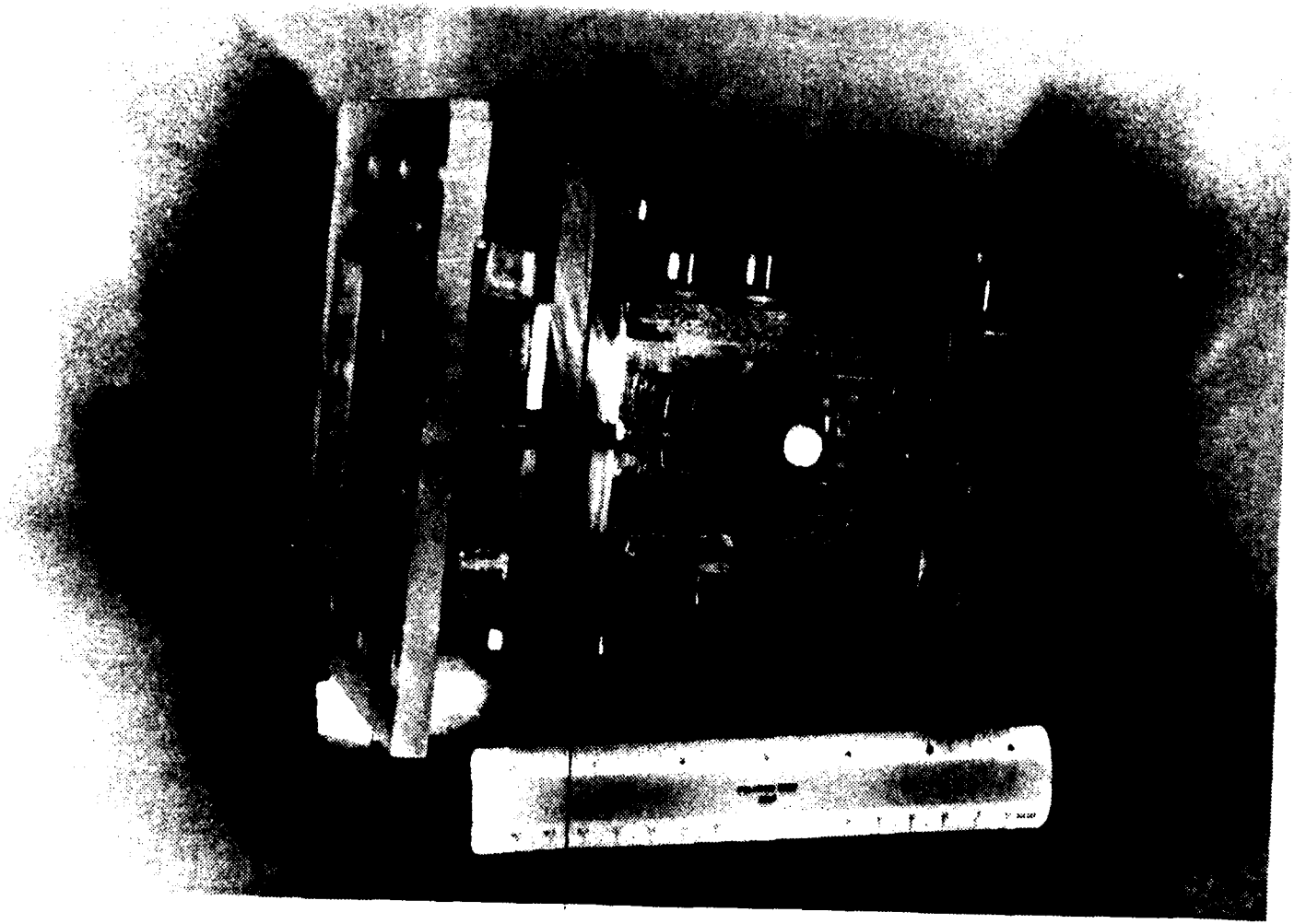

Figure 9. Parallel flow test section

Figure 10. Cross-flow test section. Anode pins visible through edge of top.

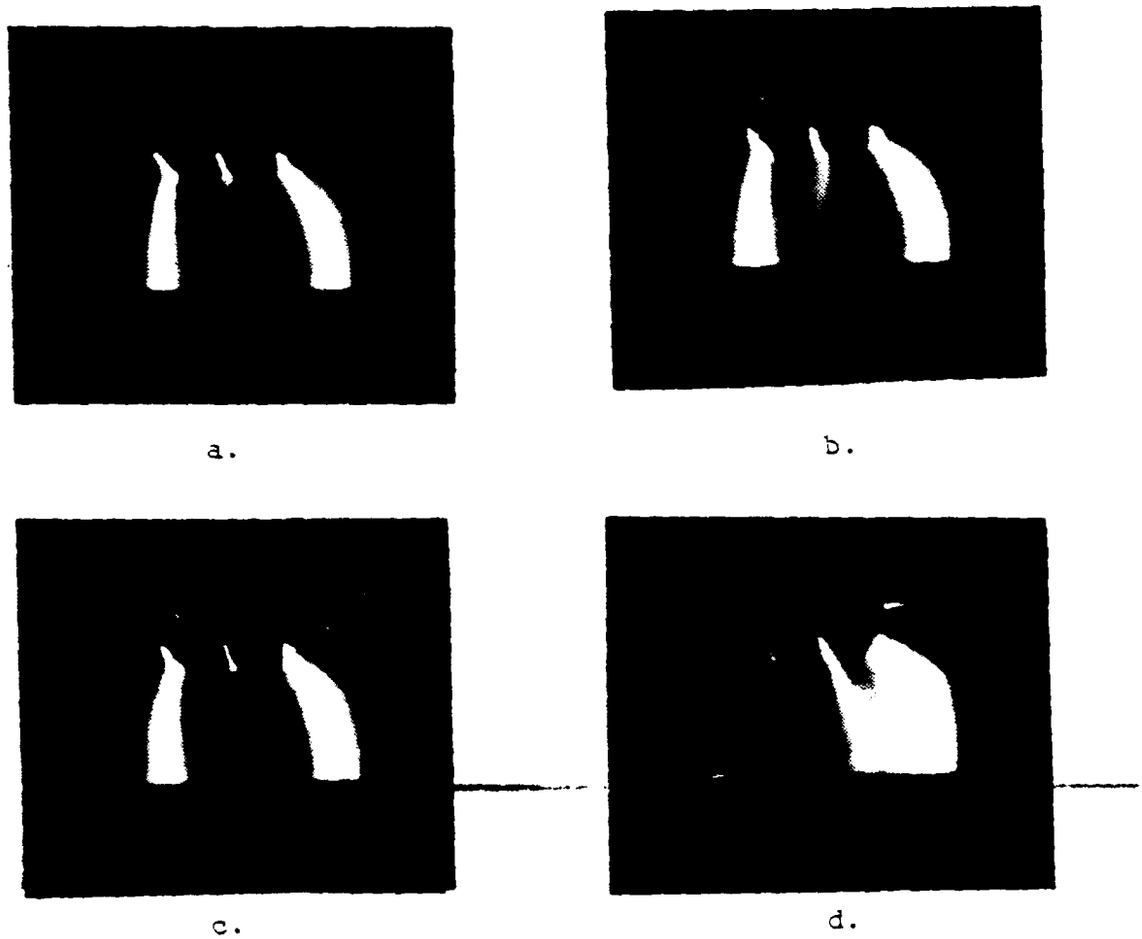

a. Flow 52.4 m/s, 21.5 kv, 1.6 ma

b. Flow 52.4 m/s, 22.0 kv, 1.5 ma total current, downstream cathode current 120 microamp

c. Flow 66.1 m/s, 22.0 kv, 1.65 ma

d. Flow 90.3 m/s, 22.0 kv, 2.4 ma

Figure 11. Cross-flow glow discharge, 2.9 cm spacing, no turbulence plate, flow from right to left.

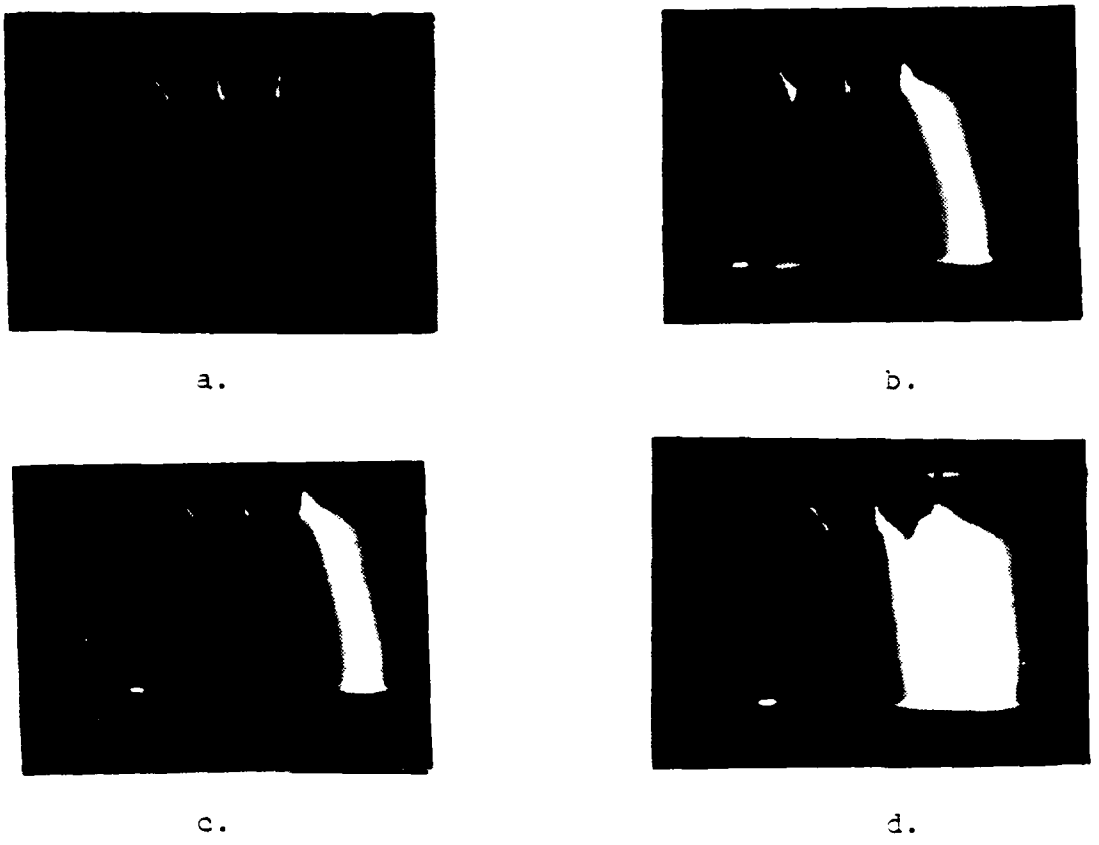

a. No-flow, 27 kv, 0.4 ma

b. Flow 52.4 m/s, 29.0 kv, 0.7 ma

c. Flow 66.1 m/s, 30.0 kv, 1.0 ma

d. Flow 90.3 m/s, 30.0 kv, 2.4 ma

Figure 12. Cross-flow glow discharge, 4.1 cm spacing, no turbulence plate, flow from right to left.

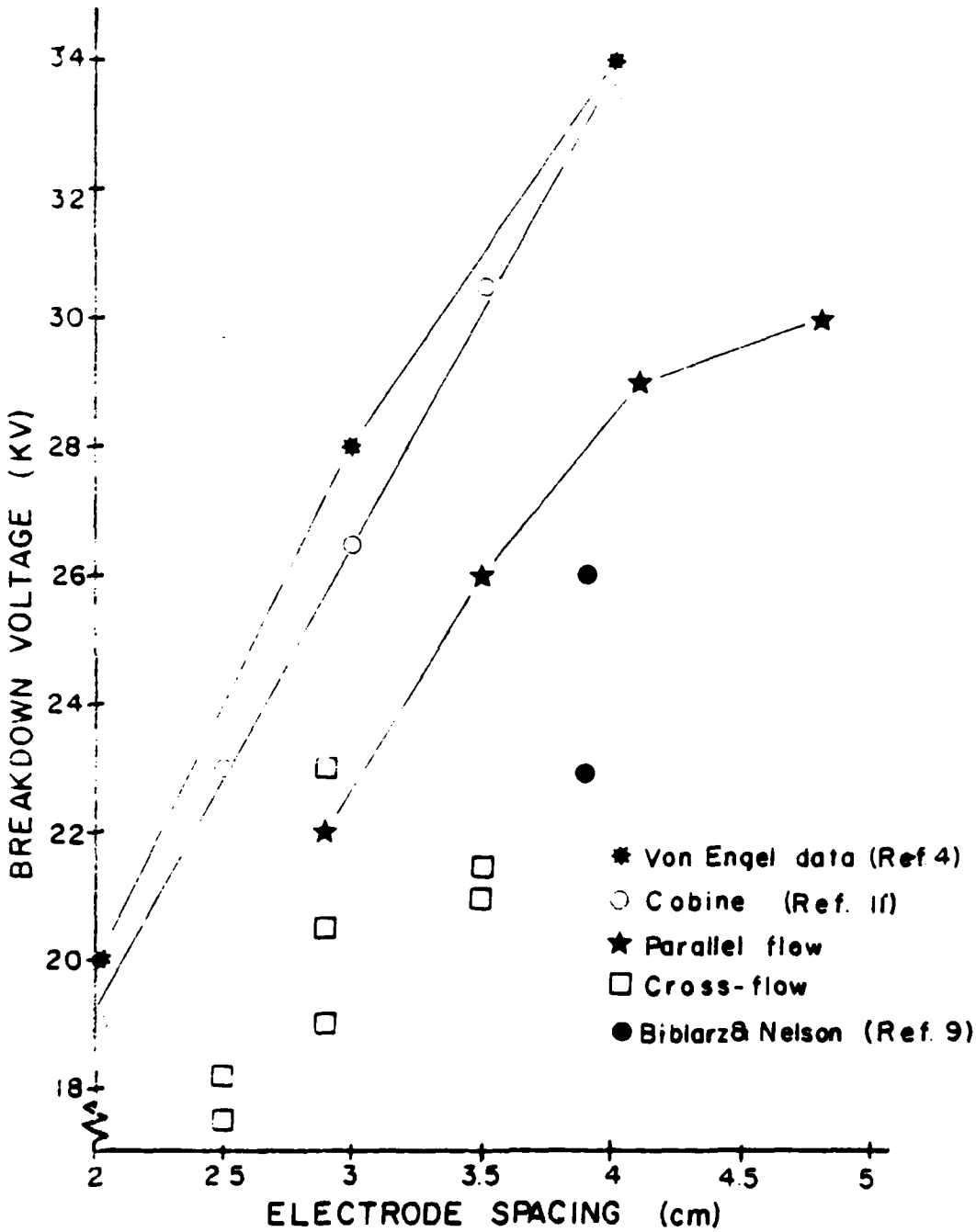


Figure 13. No-flow breakdown voltage versus spacing

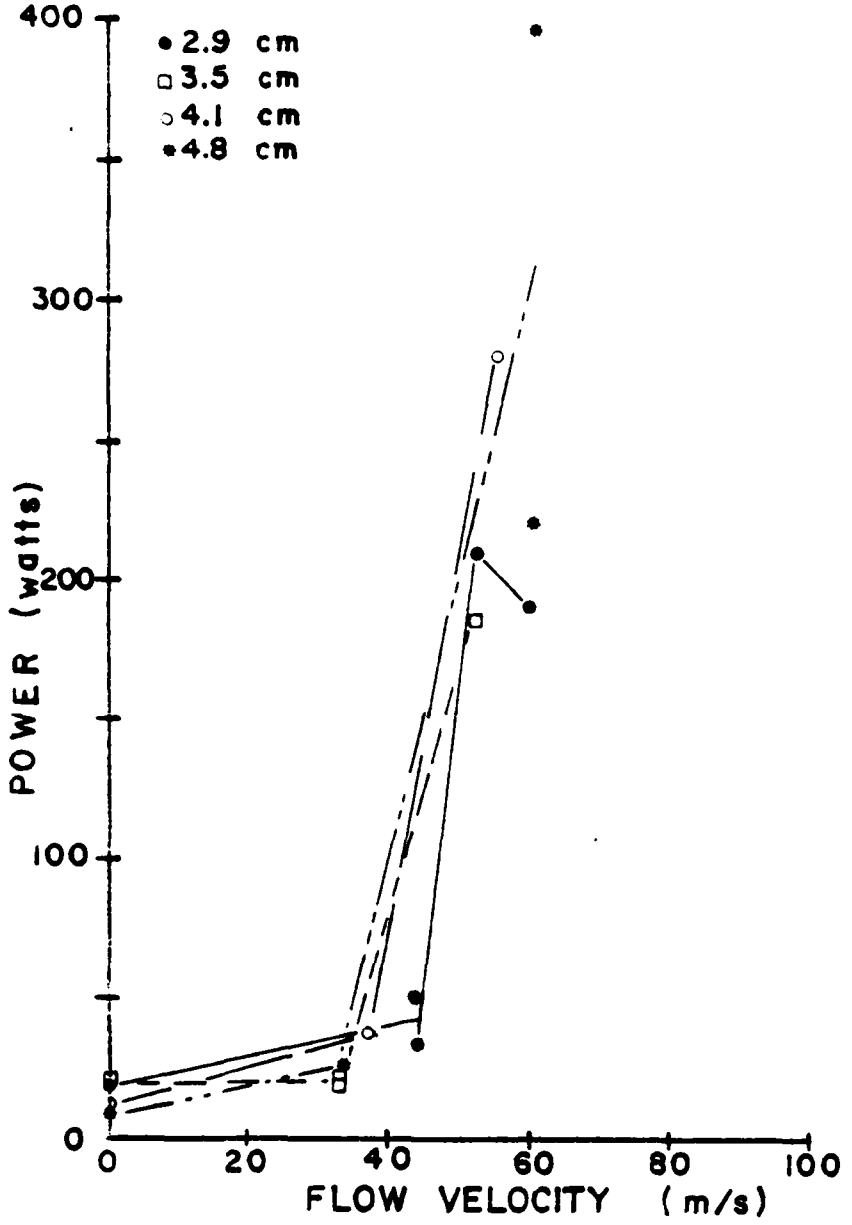


Figure 14. Parallel flow discharge power versus velocity, with turbulence.

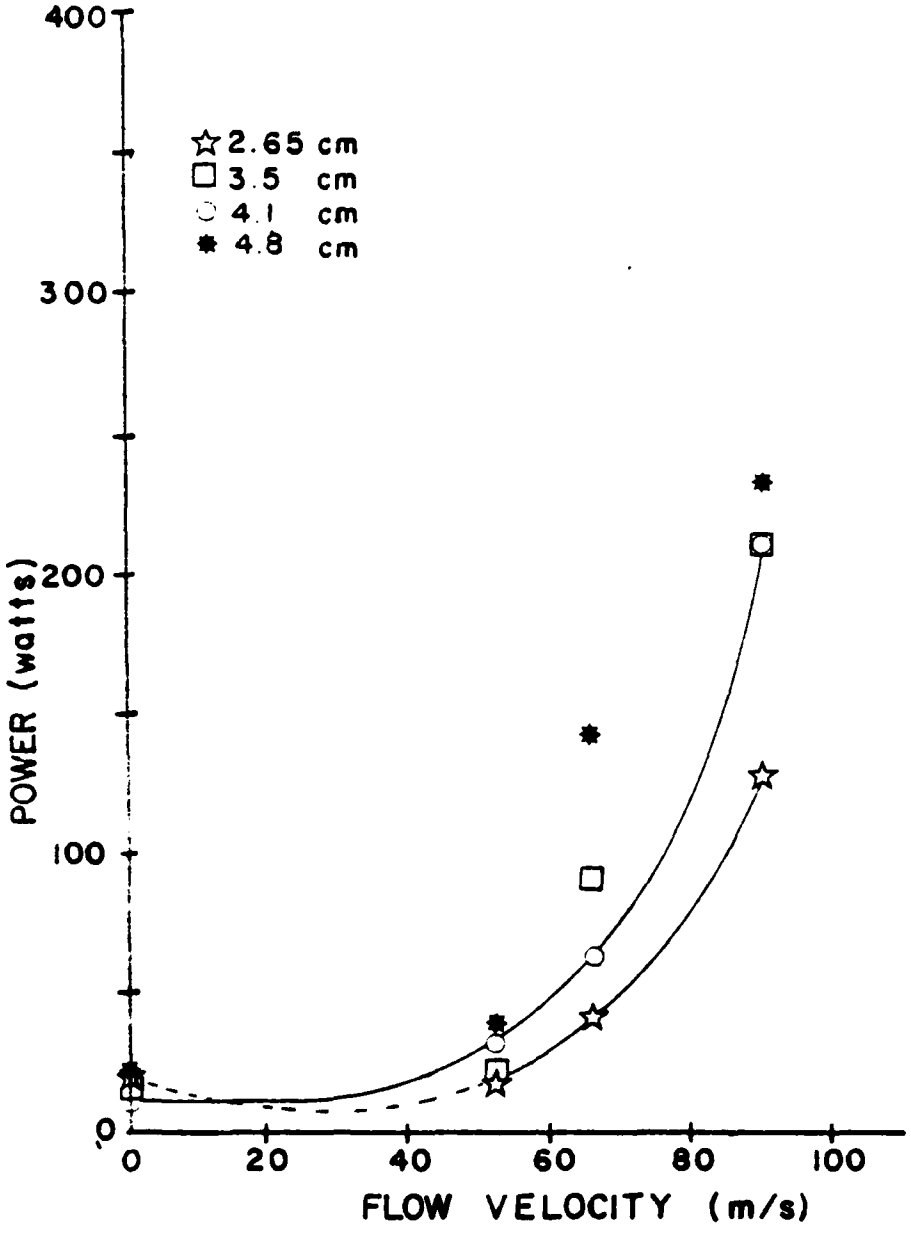


Figure 15. Parallel flow discharge power versus velocity, no turbulence.

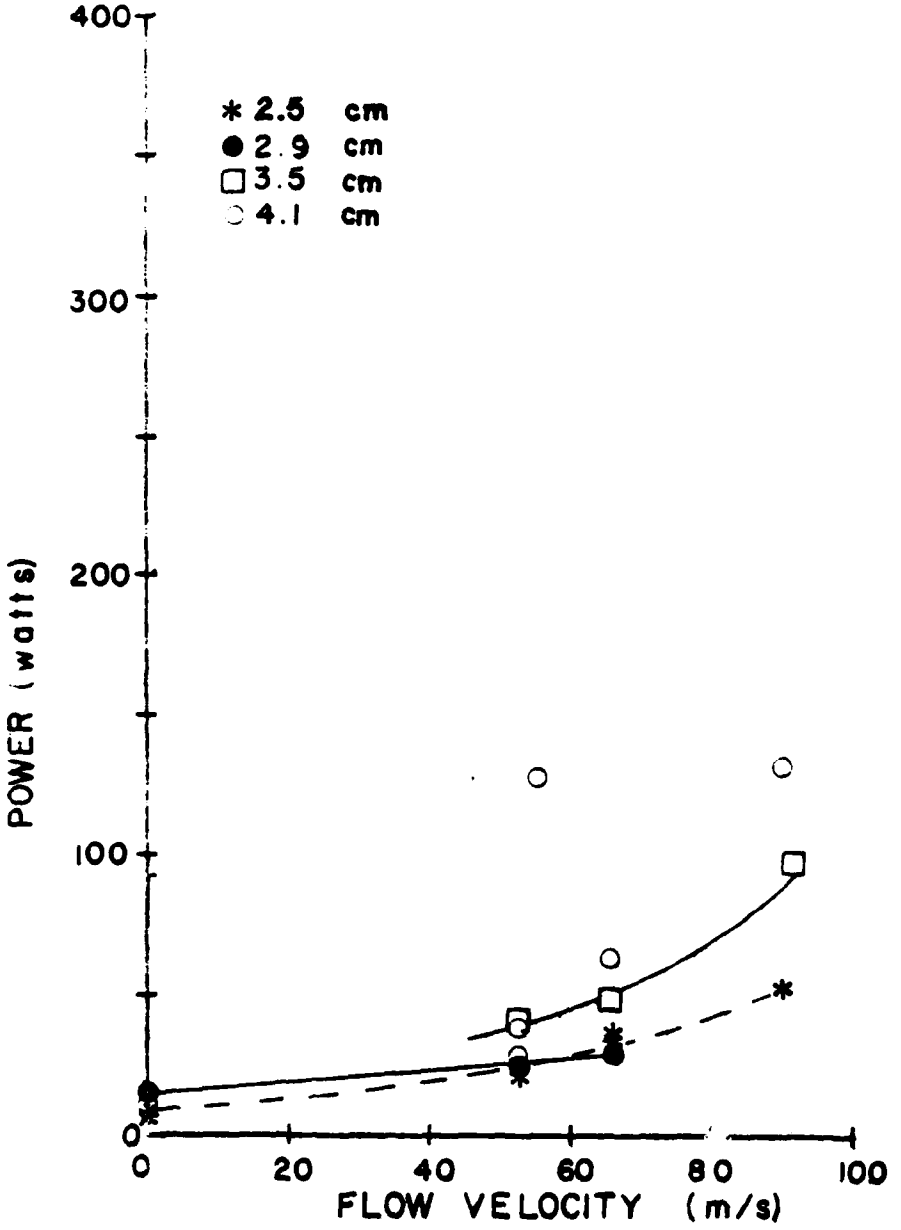


Figure 16. Cross-flow discharge power versus velocity, no turbulence (plotted to same scale as Figures 14 and 15).

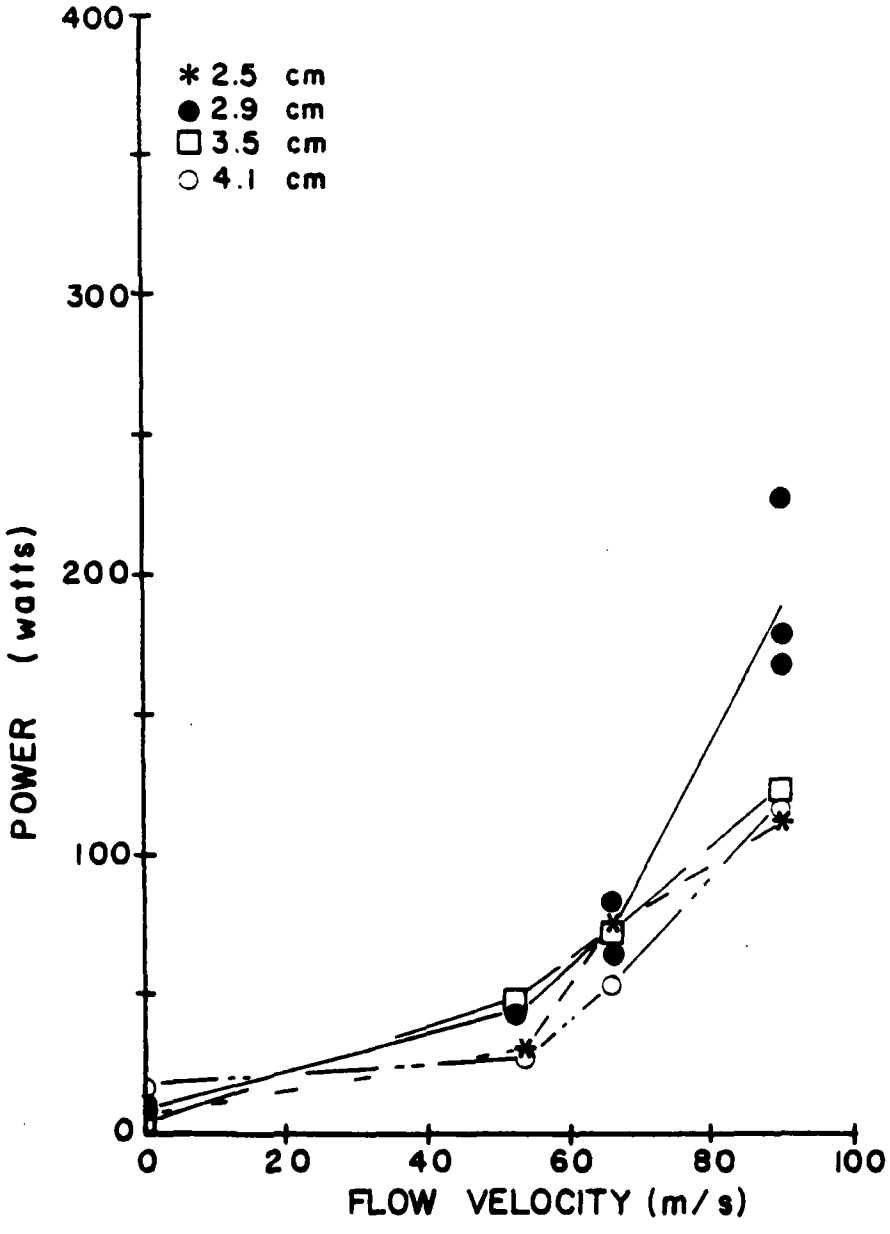


Figure 17. Cross-flow discharge power versus velocity, (with turbulence). (Plotted to same scale as Figs. 14 and 15).

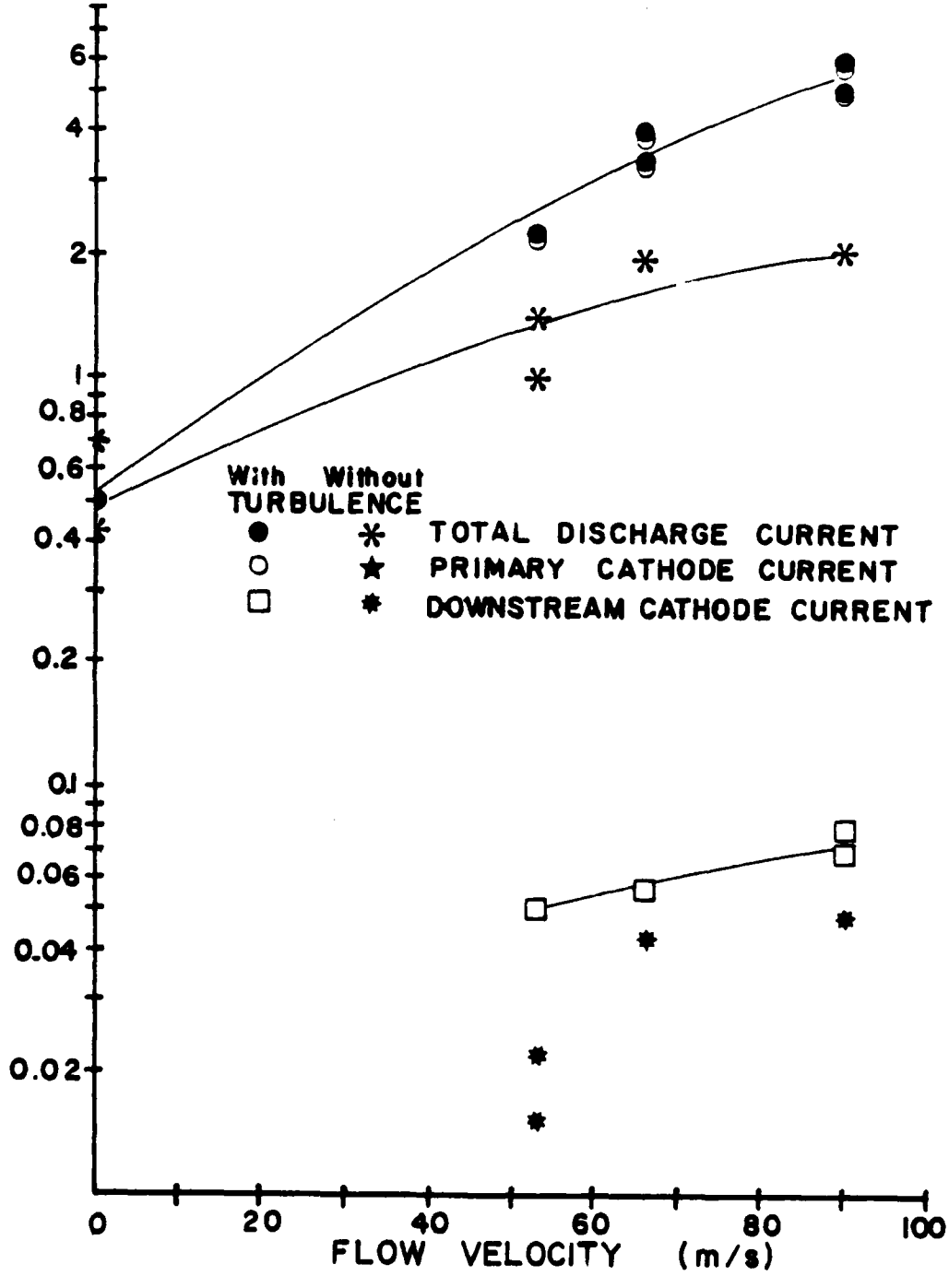


Figure 18. Breakdown current versus flow velocity, 2.5 cm, cross-flow.

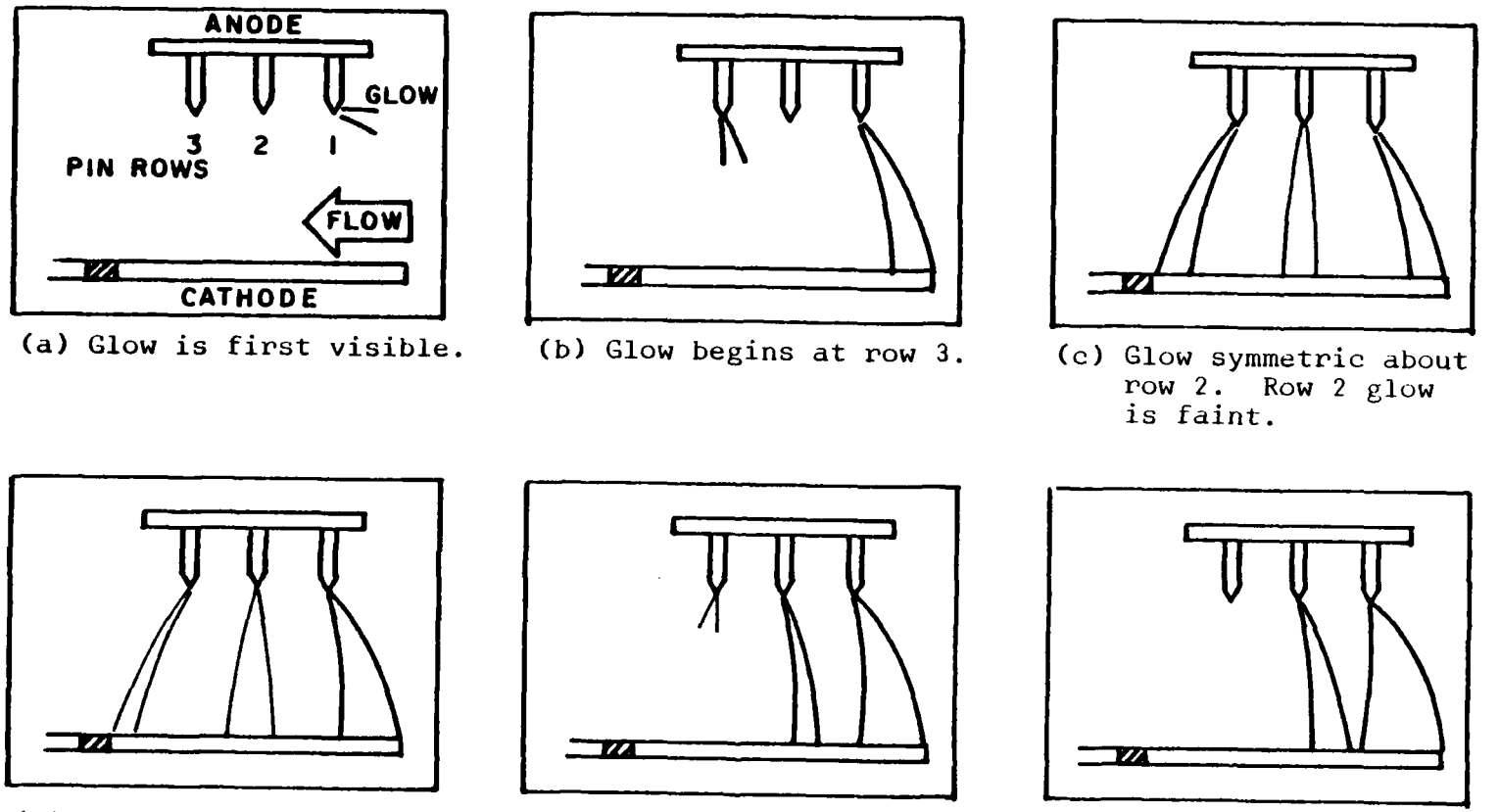


(a) Glow is first visible.

(b) Glow begins at row 3.

(c) Glow symmetric about row 2. Row 2 glow is faint.

(d) Row 1 glow widens.

(e) Row 2 glow brightens. Row 3 glow dimishes.

(f) Breakdown is impending.

Figure 19. Glow discharge variation with voltage, cross-flow configuration. Voltage increases from (a) through (f) (see text). The flow is from right to left.

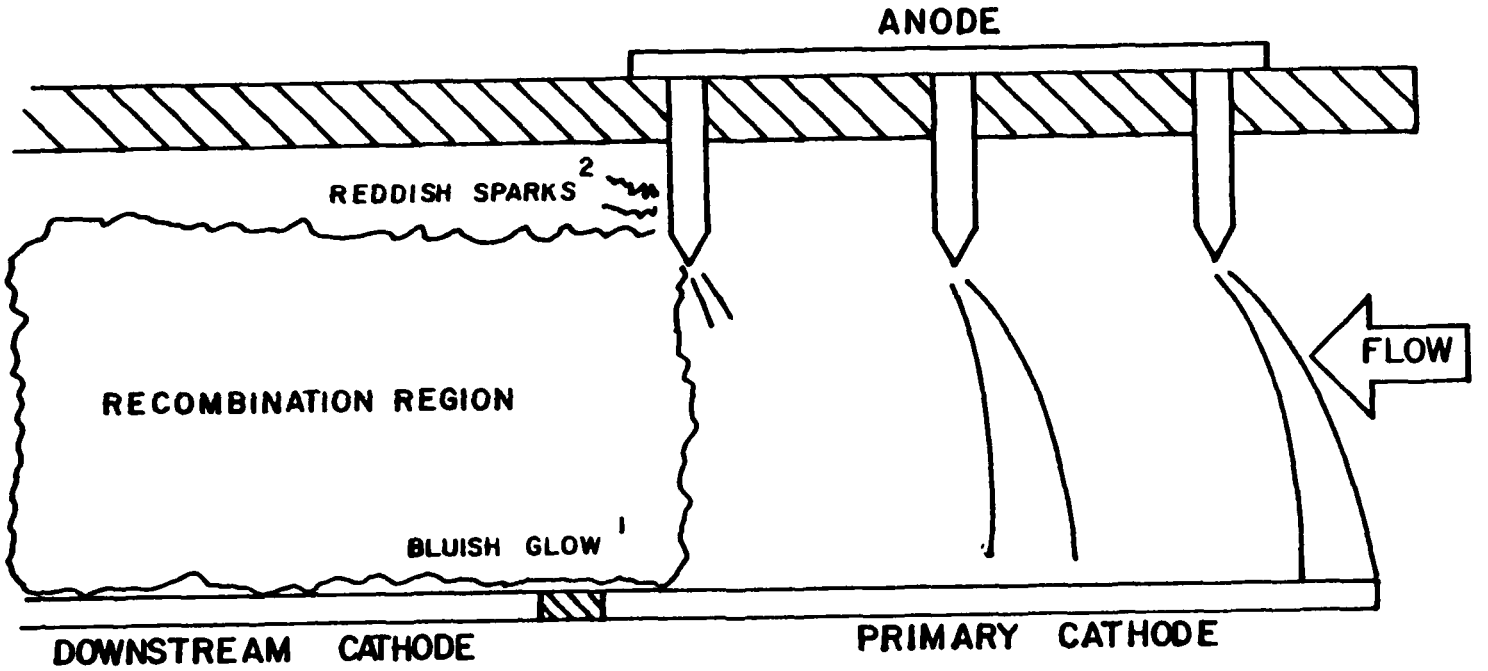


CHARACTERISTIC COLORS [Ref. 12]

| GAS | FIRST CATHODE LAYER | NEGATIVE GLOW | POSITIVE COLUMN |
|---|---|---|---|
| AIR | Pink | Blue 1 | — |
| NITROGEN | Pink | Blue 1 | Red 2 |
| OXYGEN | Red 2 | Yellow-white | Pale yellow with pink center |

Figure 20. Glow discharge sketch, cross-flow configuration.

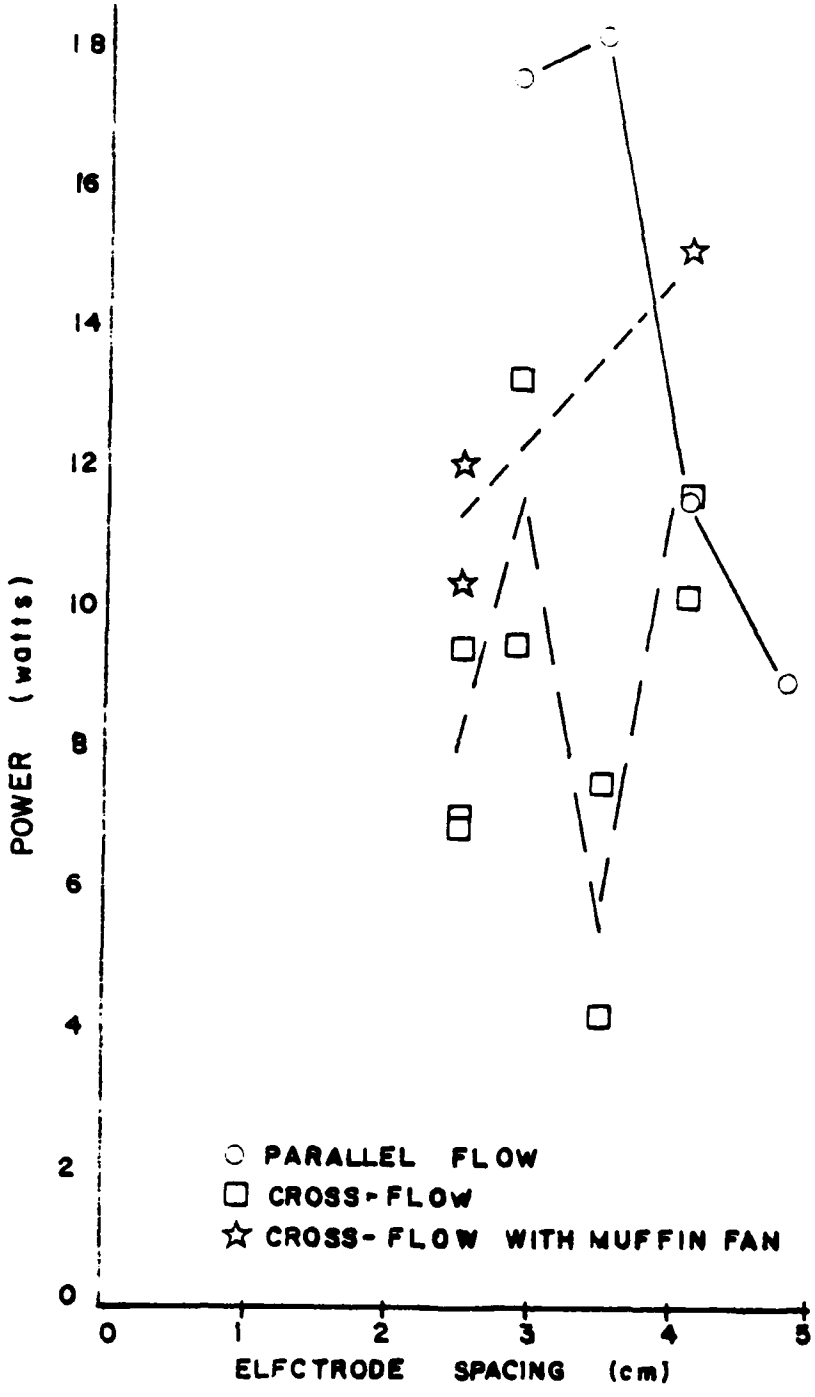


Figure 21. Power versus spacing, no flow

## REFERENCES


1. Loeb, L. B., Electrical Coronas, p. 110, University of California Press, 1965.

2. Fuhs, A. E., "High Energy Laser System Design", notes from a course in the Department of Aeronautics, Naval Postgraduate School, Monterey, California, January 1981.

3. Post, Howard A., Sub-Ambient Controlled Turbulence Effects on Discharge Stabilization for Laser Applications, MS Thesis, U. S. Naval Postgraduate School, September 1976.

4. Aunchman, Leman J., Controlled Turbulence as a Design Criterion for Electric Discharge Convection Lasers, MS Thesis, U. S. Naval Postgraduate School, March 1974.

5. Barto, Jonney L., Gasdynamic Effects on an Electric Discharge in Air, MS Thesis, U. S. Naval Postgraduate School, September 1976, also, Report NPS 67-80-005, August 1980.

6. Davis, Charles H., Aerodynamic Stabilization of an Electrical Discharge for Gas Lasers, MS Thesis, U. S. Naval Postgraduate School, March 1981.

7. Von Engel, A., Ionized Gases, Second Edition, Oxford, 1965.

8. Loeb, L. B., The Mechanism of the Electric Spark, Stanford University Press, 1941.

9. Biblarz, O., and Nelson, R. E., "Turbulence Effects on an Ambient Pressure Discharge", Journal of Applied Physics, v. 45, pp. 633-637, February 1974.

10. Biblarz, O., et al, "Gas Dynamic Effects on Diffuse Electrical Discharges in Air", Israel Journal of Technology, v. 15, pp. 59-69, 1977.

11. Cobine, J. D., Gaseous Conductors, Theory and Engineering Applications, p. 190, McGraw-Hill, 1941.

12. Nasser, Essam, Fundamentals of Gaseous Ionization and Plasma Electronics, New York, 1971.

13. Brown, Sanborn C., Introduction to Electrical Discharges in Gases, p. 214, New York, 1966.

14. Lancashire, R.B., et al, "The NASA High-Power Carbon Dioxide Laser: A Versatile Tool for Laser Applications," Optical Engineering, v. 16, No. 5, p. 506, September 1977.

15. Phelps, C. T. and Griffiths, R. J., "Dependence of Positive Corona Streamer Propagation on Air Pressure and Water Vapor Content," Journal of Applied Physics, v. 47, p. 2929, July 1976.

INITIAL DISTRIBUTION LIST

| | | No. Copies |
|---|---|---|
| 1. | Defense Technical Information Center<br>Cameron Station<br>Alexandria, Virginia 22314 | 2 |
| 2. | Library<br>Code 0142<br>Naval Postgraduate School<br>Monterey, California 93940 | 2 |
| 3. | Office of Research Administration<br>Code 012A<br>Naval Postgraduate School<br>Monterey, California 93940 | 2 |
| 4. | Chairman<br>Department of Aeronautics<br>Code 67<br>Naval Postgraduate School<br>Monterey, California 93940 | 2 |
| 5. | Professor Oscar Biblarz<br>Department of Aeronautics<br>Code 67Bi<br>Naval Postgraduate School<br>Monterey, California 93940 | 5 |
| 6. | LCDR John W. Wainionpaa, USN<br>Patrol Wing One Detachment Kadena<br>FPO Seattle, Washington 98770 | 1 |
| 7. | LCDR J. L. Barto, USN<br>Weapons Systems Officer<br>Code 2004<br>Pacific Missile Test Center<br>Point Mugu, California 93042 | 1 |
| 8. | LCDR Stephen T. Van Brocklin, USN<br>565 F Avenue<br>Coronado, California 92118 | 1 |
| 9. | Commander<br>Naval Air Systems Command<br>Department of the Navy<br>ATTN: Dr. H. R. Rosenwasser, Code AIR 310C<br>Washington, D.C. 20360 | 1 |

No. Copies

10. Mr. John A. Satkowski — 1
Office of Naval Research
Power Program, Code 473
Washington, D.C. 20360

11. Dr. William L. Nigham — 1
United Aircraft Research Laboratory
East Hartford, Connecticut 06108

12. Dr. B. N. Srivastava — 1
AVCO Everett Research Laboratory
2385 Revere Beach Parkway
Everett, Massachusetts 02149

13. Dr. J. Shwartz — 1
TRW System
One Space Park
Redondo Beach, California 90278

14. Dr. Alan Garscadden — 1
AFAPL/POD
Building 450/Room D101
Wright-Patterson AFB, Ohio 45433

15. Dr. A. V. Phelps — 1
JILA
Boulder, Colorado 80309

16. Dr. R. B. Lancashire — 1
NASA Lewis Research Center
Cleveland, Ohio 44135

END

DATE
FILMED
4-82

DTIC